

CHARTER IV

RESULTS AND ANALYSIS

The Technical Equation and Condition

1. The Experimental Evaluation

1.1 The Characteristics of Solar Radiation

The characteristics of solar radiation not only base on the geographical latitude, but also on the time of day, month and year at a given location. Because of the inclination of the earth's axis, the days in summer are longer than in winter and the sun reaches higher solar altitudes in summer than in winter period. In Figure 29, the average daily solar irradiation that struck on the horizontal plane, global radiation was 4.70 kWh.m^{-2} , the tilted plane, collector surface radiation was 5.05 kWh.m^{-2} and the average ambient temperature was $32 \text{ }^\circ\text{C}$. Only in summer, the global radiation was more than other season. Because the solar collector modules were installed on the roofs of the Testing building, they were inclined toward the south-east and the slope of 20° of the roofs. A general rule of thumb is that a solar collector should roughly face the equator and the optimal tilt angle should be close to 0.7 times the latitude, but always at least 10° or the minimum tilt angle specified for the solar collector (The German Solar Energy Society, 2005, unpagged). Figure 30 illustrated the variation of the average daily solar irradiation that struck on the collector surface by the season and time. It could receive a maximum solar irradiation at 13:00 in summer of about 900 W.m^{-2} , in winter it was about 800 W.m^{-2} and 700 W.m^{-2} in rainy season. The minimum value for the year appeared at 17:00 and was about 300 W.m^{-2} .

1.2 Efficiency of a Solar Collector

The heat transfer takes place from the collectors to the water. There is a primary cause of feeding energy through the chiller that measurement in term of solar collector efficiency. Figure 31 demonstrated that the increasing of efficiency depended on the solar radiation; thus, the energy gained of a solar thermal collector would be increased more than proportional to the solar radiation. The average daily solar collector efficiency during year 2006 was only 0.55 because the collectors were not installed in the optimum orientation.

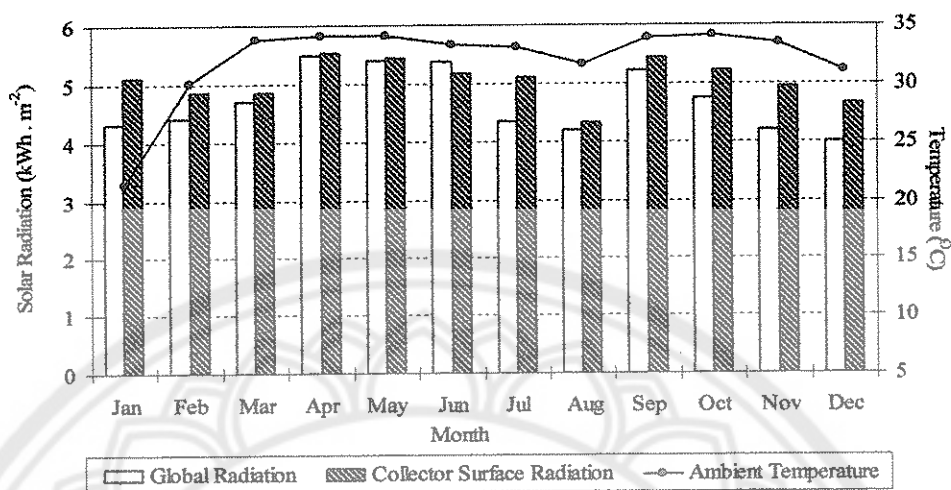


Figure 29 The average daily solar radiation that struck on horizontal, tilted plane and ambient temperature

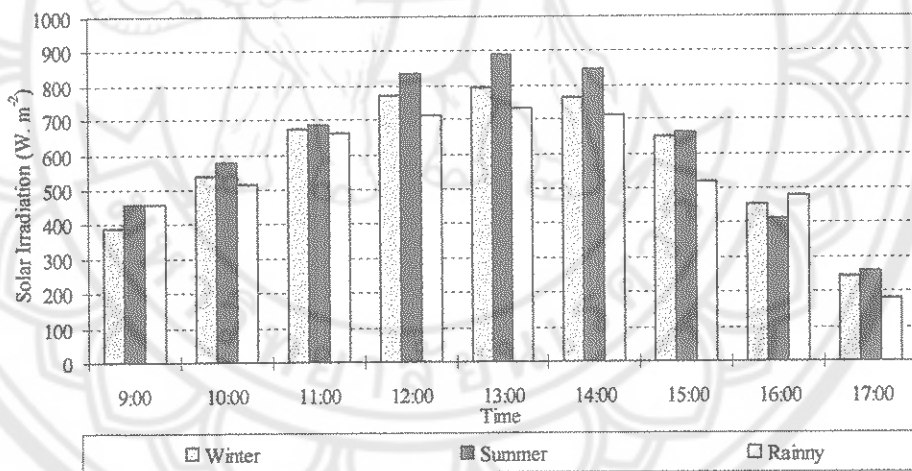


Figure 30 The average daily solar radiation that struck on collector surface versus the season in Thailand

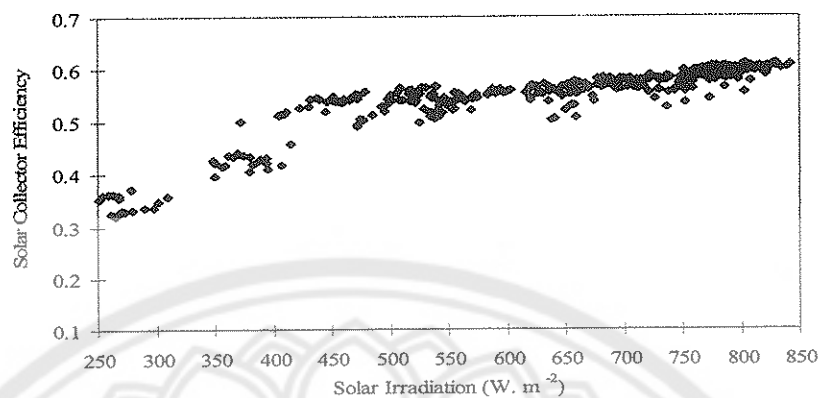


Figure 31 The average daily solar collector efficiency versus solar irradiation

1.3 The Underwent Parameters

The solar irradiation that struck on collector surface was increasing. The parameters which underwent significant variation were the driving temperature and useful temperature when the sun was rising. In Figure 32, in winter, while the beginning temperature was 50 °C, the highest peak of the sun could generate the average temperature of working fluid for driving and usage was 79 °C and 5 °C, respectively. In March, the daily average of working fluid for the driving temperature starting from 55 °C through the temperature was 75 °C and the useful temperature was 15 °C on the highest peak of solar radiation in Figure 33. The scattering of solar radiation was found in Figure 34 because it was beginning of rainy season while the starting temperature was 35 °C. The daily average of driving temperature and the useful temperature of water was 70 and 15 °C, respectively.

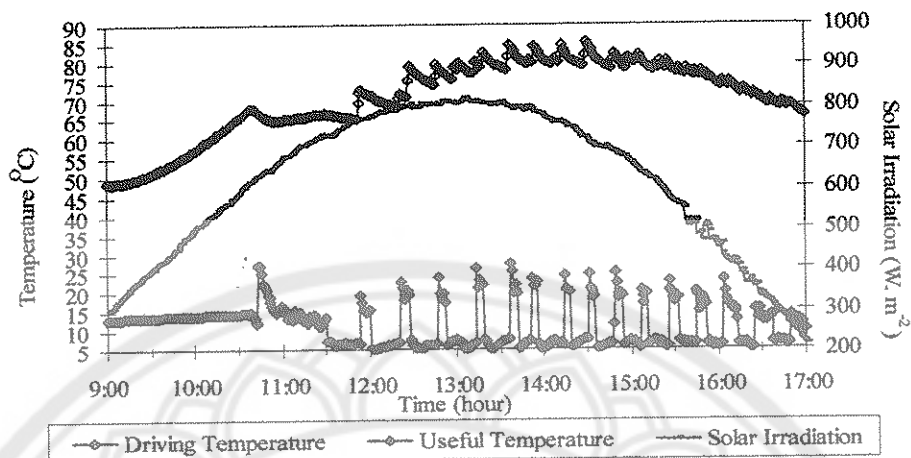


Figure 32 Working fluid temperature, water, versus solar irradiation that measurement on February

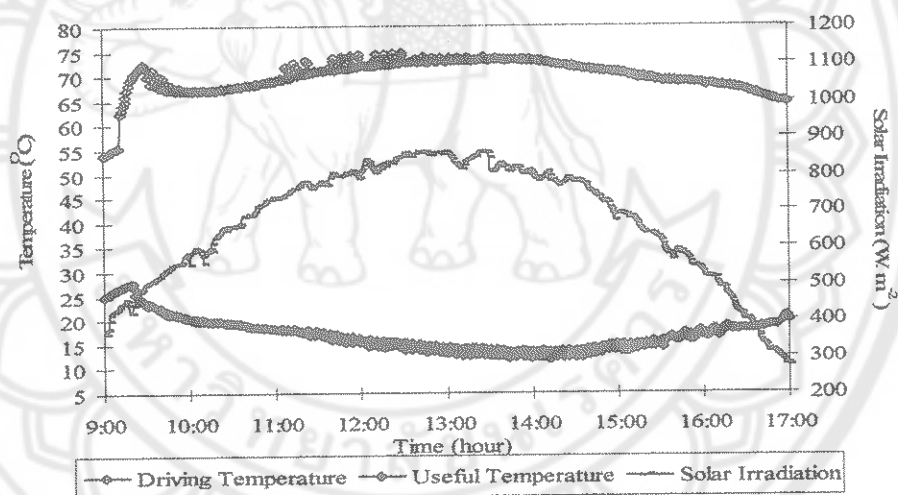


Figure 33 Working fluid temperature, water, versus solar irradiation that measurement on March

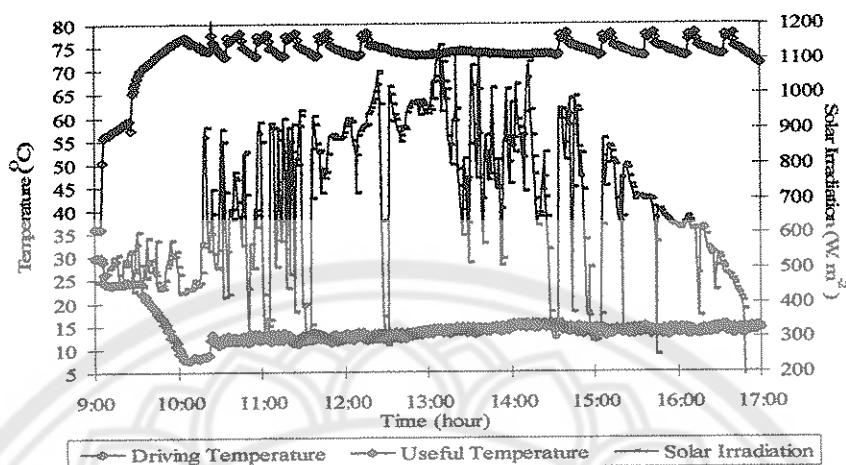


Figure 34 Working fluid temperature, water, versus solar irradiation that measurement on July

1.4 Auxiliary Heat Consumption

The auxiliary heat source needs to assure that solar-assisted air-conditioning system always had been enough heat available to meet the load. The total energy supply to the absorption chiller was the summation of solar thermal and auxiliary heat could write as solar fraction that described as the ratio of solar heat yield to the total requirement for hot water heating. The higher of solar fraction caused the lower amount of energy required for auxiliary heating. Figure 35 showed the daily average solar fractions for this machine in a temperate climate. It could be seen the range of average daily solar fraction ranging 0.4 to 0.7 during the operation period. As the feeding water flow rate was fixed, the significant temperature variation was detected at the evaporator that formed the cooling load. It had to be discharged by the fan coil units to maintain the desired room temperature, affected by the solar irradiation that strike on the collector surface.

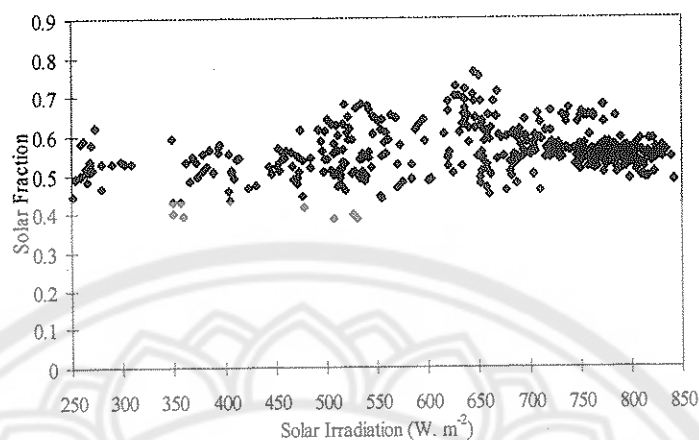


Figure 35 The average daily solar fraction versus solar irradiation

1.5 Cooling Capacity and Balancing Energy

Figure 36 presented the average daily cooling capacity that generated by working of chiller during year 2006 was 15 kW while the average daily solar irradiation was 600 W.m⁻². Of course, one of the most important measurements was the balancing of the energy supply and energy demand. In Figure 37, the absorption chiller demand contributed of the solar collector array and auxiliary heater supply. As expected, in Thailand during winter and summer were the best contributions from the collector array. Meanwhile, during Thailand's rainy season, when it was cloudy, the collector array energy supply dropped. In winter, the daily average of chiller demand, 168.07 kWh, was balanced by the daily average of collector and heater supply was 247.67 and 170.56 kWh, respectively. The highest of the average collector supply appeared on summer was 288.64 kWh and the heater supply was 128.94 kWh to meet the daily average of demand was 115.51 kWh. Increasing of average daily cooling demand, 100.20 kWh, during rainy season effected on the daily average of heater supply, 161.92 kWh, with the lowest daily average of collector supply was 186.14 kWh. The discrepancy between the large collector array supply differenced from month to month and the relatively small absorption chiller energy demand results was in a large increase in auxiliary heater supply during the year. Nevertheless, it should keep in mind that this condition was depend on the balancing of cooling demand and supply such as the lowest cooling demand appeared on summer because of a few activity generated owing to long holiday in Thailand.

1.6 The Actual COP

The rating supplied by the manufacturer showed a COP at nominal conditions equal to 0.70. In Figure 38, the measurements showed values of the average daily actual COP was 0.30. It was consistent increasable versus the average irradiation during the year. The measurement showed the main factor that affected the balancing and COP of chiller was the energy demand during the year. Different activities generated various demands or cooling load such as the long holiday effected on the lowest cooling load that appeared in summer. Figure 39 showed a comparison between the average daily maximum and minimum actual COP variation of seasonal condition. The most differential value was found in the summer, the maximum value was 0.46 while the minimum was 0.11 that was generating a negative effect on the actual COP. On the other hand, the different value in winter, the maximum value was 0.60 and the minimum was 0.27 that was generating a positive effect on the actual COP due to a fewer different value.

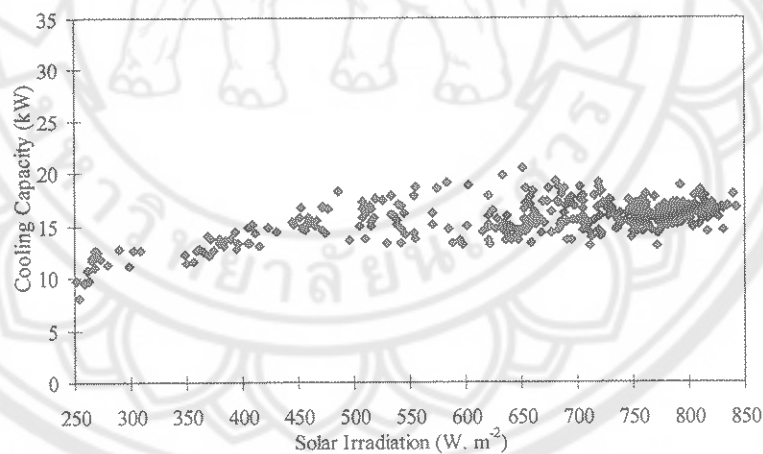


Figure 36 The average daily cooling capacity versus solar irradiation

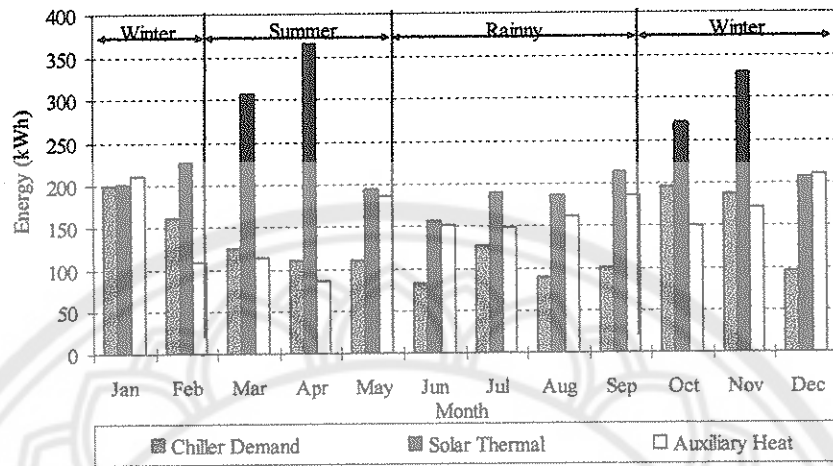


Figure 37 Energy balance for absorption chiller when operated cooling system

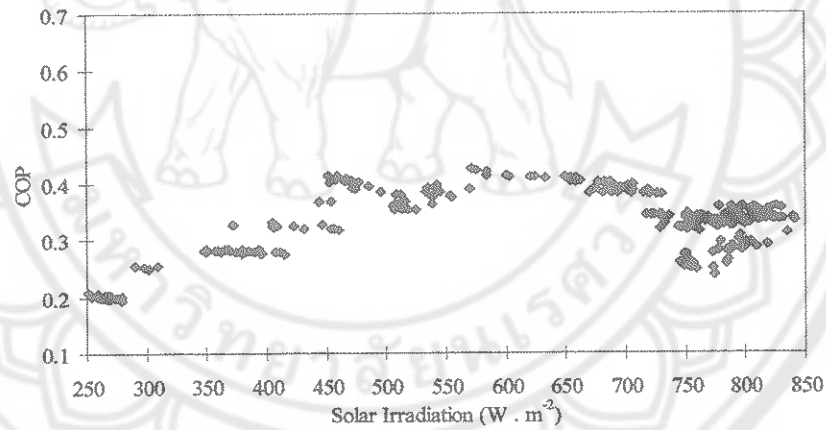


Figure 38 The average daily Coefficient Of Performance (COP) versus solar irradiation

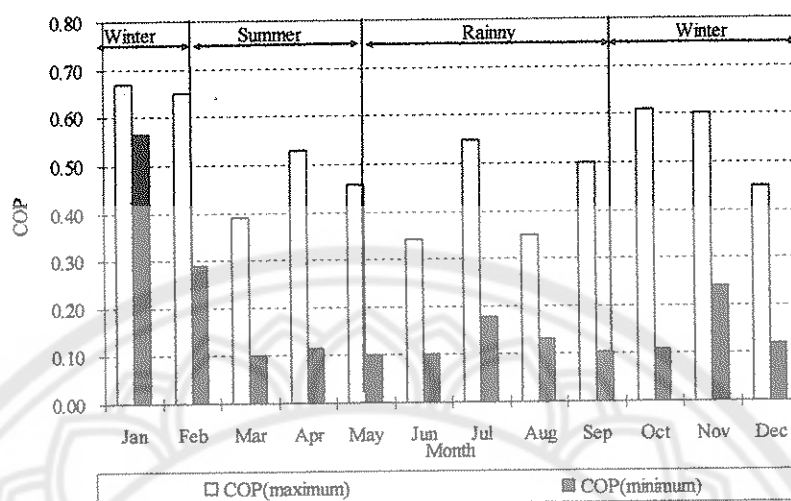


Figure 39 The average daily Coefficient Of Performance (COP) versus seasonal condition

1.7 Experimental Discussion and Outlook

The poor performance of the cooling system was partly due to the huge heat losses that observed from the unbalancing between demand and supply. This condition should be reduced by some improvements that had been made in past three decades on the main components of the solar absorption cooling system, such as the solar collector, absorption chiller and hot water storage tank (Li and Sumathy, 2001, pp. 131-138). In Figure 37, the average daily solar energy supply was overfilling when compared with the average daily chiller demand, although the collector's orientation was facing the wrong direction and slope, so the suggestion was about the chiller and the storage tank. Then, the improvements were appeared because of a low supplying temperature ranging from 60 to 75 °C. The first idea was to create a new type of cooling machine that would be more suitable to make used of the low density, unsteady solar energy, under the local climatic conditions which could be easily provided by conventional solar hot water system. The strategy of absorption cooling developed to provide a more efficient and cost effective solution by two-stage LiBr-H₂O absorption chiller that was expected to use less expensive models of solar collectors (Sumathy, Huang and Li., 2002, pp. 155-165). The second idea was to increase the size and the height of hot water storage tank that usually be improved

storage for hot and cold water depending on the load (Oppel, Ghajar, and Moretti, 1986, pp. 293–309). Improving the positive of performance for the entire solar cooling by an appropriate design was the thermally stratified storage tank. This natural process created a transition zone temperature gradient between cold and hot fluid zones, called the thermocline (Abdoly and Mohammad, 1981, unpagged). Thermocline storage was attractive because the working fluid could be sent to the solar collector at lower temperature. The potential reduction in cost and complexity of pumping, valving, and pumping also make it highly desirable to investigate at some length of the characteristics and behavior of the storage system. For temperature stratified water tank was limited by the flow rate, collector flow and load flow (Li and Sumathy, 2002, pp. 1207-1216).

This experiment had a limitation of water flow rate via the four main flow circuits would have significantly affect the thermal energy that is balancing the COP, whereas measurements taken by other works (Yongprayun, Ketjoy and Rakwichian, 2006, pp. 1-5). It indicated that the supplying water temperature effects on the actual COP by varying the flow rate, as measurements taken by other author (Aadrubali and Grignaffini, 2005, pp. 489-497; Mittal, Kasana, Thakur, 2005, unpagged; Kaynakli, and Kilie, 2007, pp. 599-607). On the other hand, increasing the frequency of cleaning the solar collector and cooling tower which was an effect of operating conditions (Bhadania, Shah, Upadhyay, Shah, and Patel, 2003, unpagged), was just as important as the frequency of examining and repairing the pipe's joint in order to reduce the heat losses in the water circuit and improve the efficiency of the components (Ardehali, Shahrestani and Adams, 2007, pp. 489-497).

2. The System Equation

2.1 The Results of System's Equation

Data in Table 4 was written in the linear function. Most equations were written in the relation between G_{β} and \dot{Q} as x and y of linear function because of the ΔT was related with \dot{m} in the sensible heat equation, Eqs. (3-11), (3-12), (3-13), (3-14), and (3-15). For the first equation, the slope always was 0.05 that generated the reduction of beginning of $\dot{Q}_{collector}$ was -3.56, -2.49, and -3.65 kW when it was running in the winter, summer and rainy season, respectively. For the second equation, the

slope value in winter, summer and rainy season was 0.03, 0.02, and 0.002, respectively, could generate the started heat form collector, \dot{Q}_1 , was -3.48, 1.63, and 16.33 kW, respectively. From this action, the beginning \dot{Q}_{gen} was -4.19, -0.17, and 18.98 kW with the slope was 0.05, 0.02, and -0.001 when G_β was run in each season. The linear function between G_β and \dot{Q}_{evap} , the slopes' values was 0.02, 0.02, and 0.002 when the cooling capacity was started from -5.06, -5.02, and 13.60 kW in winter, summer and rainy season, respectively. For the heat rejected equations, the rising of \dot{Q}_{rej} could produced by the slope was 0.05, 0.02, and 0.002 when the G_β was run while the beginning of \dot{Q}_{rej} was 20.05, 18.96, and 37.17 kW in each season. The rising of $\dot{Q}_{auxiliary}$ was due to the running of G_β with the slope was 0.0001 and the started $\dot{Q}_{auxiliary}$ was 2.92 kW. The thermal performance of the operation in winter, summer and rainy season was begun from 0.27, 0.30, and 0.67, when the G_β was run with the slope was 0.0005, 0.0002, and -0.0002, respectively. The relationship between G_β and COP also found in this table, the beginning COP was 0.27, 0.30 and 0,67 while the slope was 0.0005, 0.0002 and -0.0002 in winter, summer and rainy season, respectively.

2.2 Discussion and Outlook for System's Equation

Some notices had been gotten from this equation; the first was the written linear equation between G_β and $\dot{Q}_{collector}$ in each season. Almost beginning of $\dot{Q}_{collector}$ was minus by mean of the loss that was appeared in this section due to the orientation and environment condition surrounding of solar collector. However, the performance of the collector was not change by mean of the equability of slope in each equation, so the conclusion for this equation on Table 4 was the supplying heat had a little differential in each season. The second was the beginning of \dot{Q} of the main section; the supply by mean of \dot{Q}_1 and \dot{Q}_{gen} , the demand, \dot{Q}_{evap} , the reject, \dot{Q}_{rej} , and the performance, COP, in rainy season was higher than the others. Because of the auxiliary usage could rise up the \dot{Q} and COP, nevertheless it should be turn off when the noon came. That was the reason why the slope always minus for this condition. The conclusion in this situation was the use of auxiliary could generate higher \dot{Q} and COP although the slope was minus while the G_β was running, but it was the least values

when comparisons with the beginning done. The \dot{Q}_1 and \dot{Q}_{gen} in summer were higher than winter because of the different climate condition affect to \dot{Q} and COP. Therefore, the conclusion of this situation was if the auxiliary heat was not enough or avoid for using, the climate condition will be the main factor for \dot{Q} and COP when the water flow rate was fixed. The mathematic function that come from the Least Square Method had been shown the characteristic of \dot{Q} and COP of solar cooling system when the G_β was run with the fixed flow of water in the operated condition as a x-ray image to find out the strong and weak points of this system.

Table 4 The mathematic functions of solar cooling system

Auxiliary Usage Rainy Season	Non – Auxiliary Usage	
	Winter	Summer
Supply	Supply	Supply
$\dot{Q}_{collector} = -3.65 + 0.05G_\beta$	$\dot{Q}_{collector} = -3.56 + 0.05G_\beta$	$\dot{Q}_{collector} = -2.49 + 0.05G_\beta$
$\dot{Q}_1 = 16.33 - 0.002G_\beta$	$\dot{Q}_1 = -3.48 + 0.03G_\beta$	$\dot{Q}_1 = 1.63 + 0.02G_\beta$
$\eta_{stroage} = 9.2806 - 0.011G_\beta$	$\eta_{stroage} = 0.3217 + 0.0003G_\beta$	$\eta_{stroage} = 0.2955 + 0.0003G_\beta$
$\dot{Q}_{auxiliary} = 2.92 + 0.0001G_\beta$	$\dot{Q}_{auxiliary} = \text{Non considering}$	$\dot{Q}_{auxiliary} = \text{Non considering}$
$\dot{Q}_{gen} = 18.98 - 0.001G_\beta$	$\dot{Q}_{gen} = -4.19 + 0.05G_\beta$	$\dot{Q}_{gen} = -0.17 + 0.02G_\beta$
Demand	Demand	Demand
$\dot{Q}_{evap} = 13.60 - 0.002G_\beta$	$\dot{Q}_{evap} = -5.06 + 0.02G_\beta$	$\dot{Q}_{evap} = -5.02 + 0.02G_\beta$
Reject	Reject	Reject
$\dot{Q}_{rej} = 37.17 + 0.002G_\beta$	$\dot{Q}_{rej} = -5.05 + 0.05G_\beta$	$\dot{Q}_{rej} = 18.96 + 0.02G_\beta$
Performance	Performance	Performance
$COP = 0.67 - 0.0002G_\beta$	$COP = 0.27 + 0.0005G_\beta$	$COP = 0.30 + 0.0002G_\beta$

Table 5 The relative error of the equation

Auxiliary Usage Rainy Season	Non – Auxiliary Usage	
	Winter	Summer
Supply	Supply	Supply
$\dot{Q}_{collector} = f(G_{\beta}) = -1.83\%$	$\dot{Q}_{collector} = f(G_{\beta}) = -3.55\%$	$\dot{Q}_{collector} = f(G_{\beta}) = -2.74\%$
$\dot{Q}_1 = f(G_{\beta}) = 3.57\%$	$\dot{Q}_1 = f(G_{\beta}) = 10.36\%$	$\dot{Q}_1 = f(G_{\beta}) = 1.68\%$
$\eta_{storage} = f(G_{\beta}) = 4.08\%$	$\eta_{storage} = f(G_{\beta}) = 3.22\%$	$\eta_{storage} = f(G_{\beta}) = 3.08\%$
$\dot{Q}_{auxiliary} = f(G_{\beta}) = 11.72\%$	$\dot{Q}_{auxiliary} = \text{Non considering}$	$\dot{Q}_{auxiliary} = \text{Non considering}$
$\dot{Q}_{gen} = f(G_{\beta}) = -8.69\%$	$\dot{Q}_{gen} = f(G_{\beta}) = 8.70\%$	$\dot{Q}_{gen} = f(G_{\beta}) = 8.42\%$
Demand	Demand	Demand
$\dot{Q}_{evap} = f(G_{\beta}) = -5.16\%$	$\dot{Q}_{evap} = f(G_{\beta}) = 12.48\%$	$\dot{Q}_{evap} = f(G_{\beta}) = -3.42\%$
Reject	Reject	Reject
$\dot{Q}_{rej} = f(G_{\beta}) = -0.30\%$	$\dot{Q}_{rej} = f(G_{\beta}) = 11.05\%$	$\dot{Q}_{rej} = f(G_{\beta}) = -3.03\%$
Performance	Performance	Performance
$COP = f(G_{\beta}) = 3.43\%$	$COP = f(G_{\beta}) = 10.79\%$	$COP = f(G_{\beta}) = -0.66\%$

3. The Validation Equation

The validation by relative error showed on Table 5, due to the basic assumption for this work was the relative error obtained being less than 15% (in the worst case) that make the idea to set the mathematic function into two groups and three characteristics as shown on Table 5. The Table 5 showed the relative error of equation that used Least Square to find out the relationship of x and y from the real data after analyzed by the principle equation as shown on Table 4. All equations was pass the validation for this work , then the equation after validated with relative error could be written in form of SIMULINK, MATLAB, in winter, summer, and rainy season in Figure 40, 41, and 42, respectively. It showed the system image when the G_{β} was run as a input of model with the fixed flow of water in the operated condition.

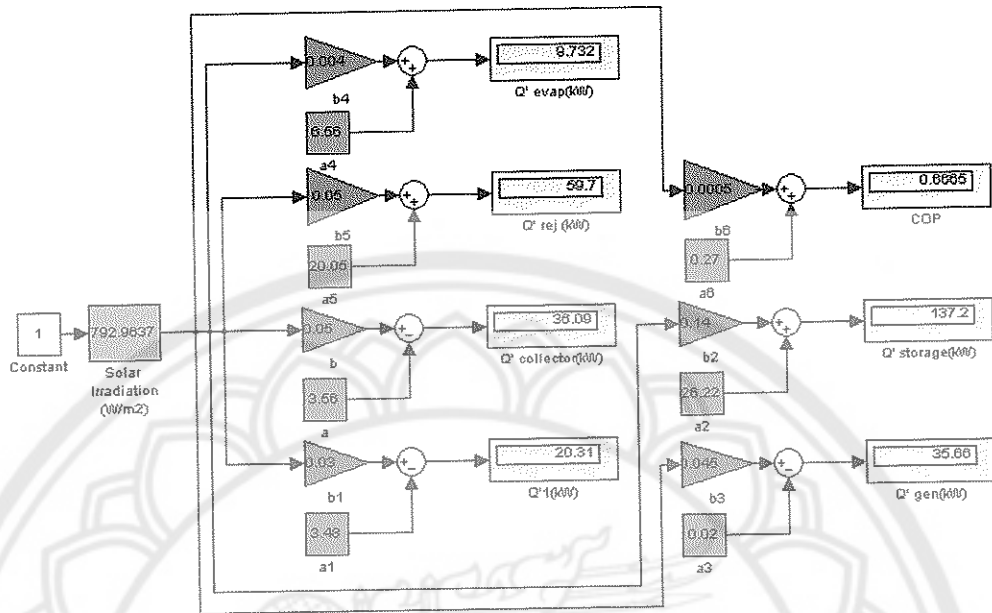


Figure 40 The mathematic model of 35 kW solar cooling that operated during the winter

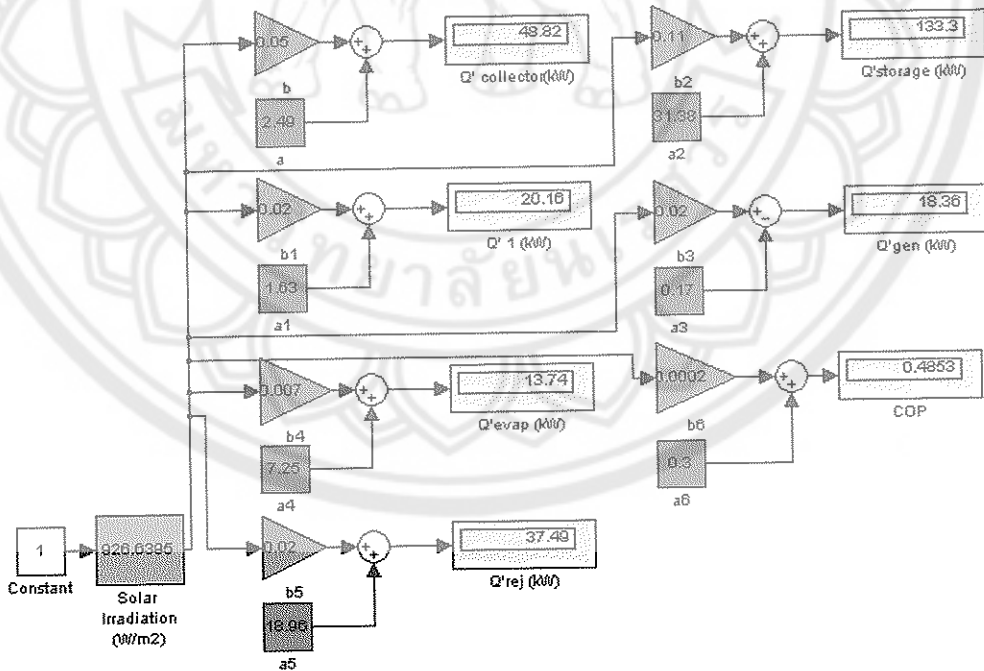


Figure 41 The mathematic model of 35 kW solar cooling that operated during the summer

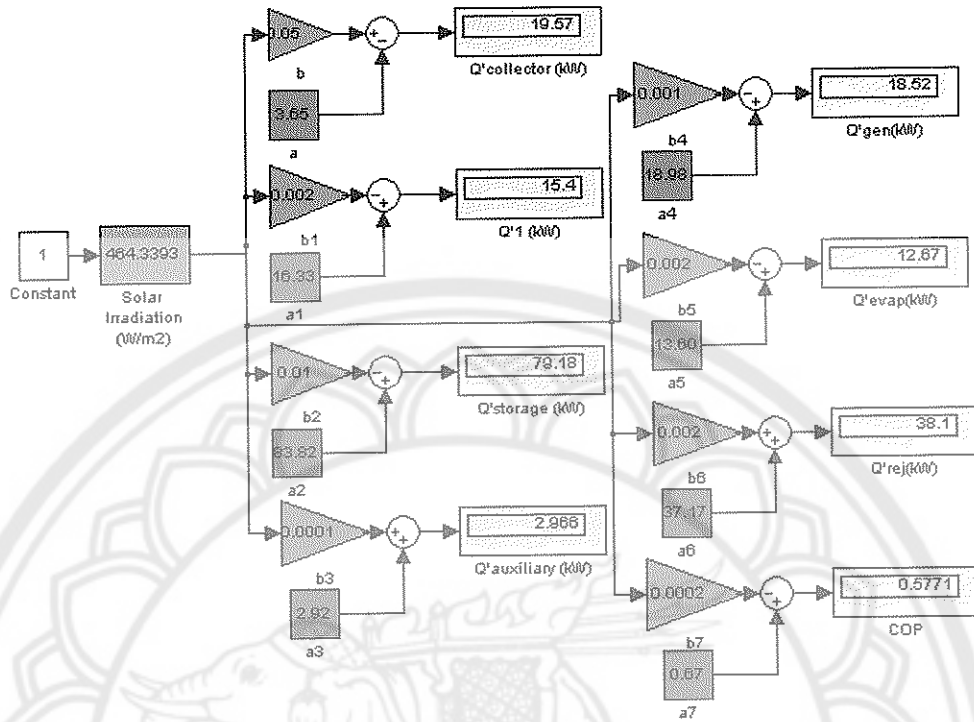
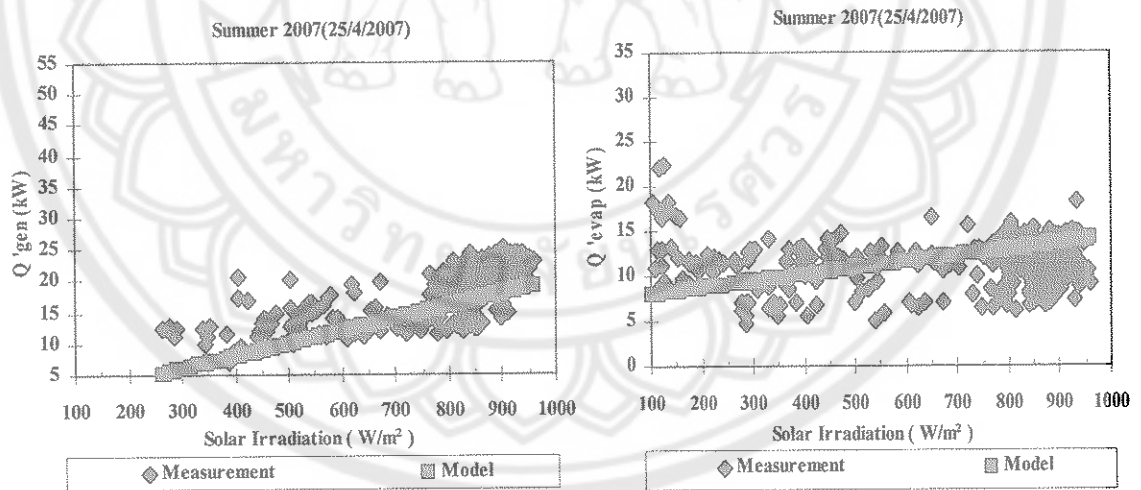


Figure 42 The mathematic model of 35 kW solar cooling that operated during the rainy season



(a) generator

(b) evaporator

Figure 43 The result of running model with the fixed flow of water in the operated condition during summer.

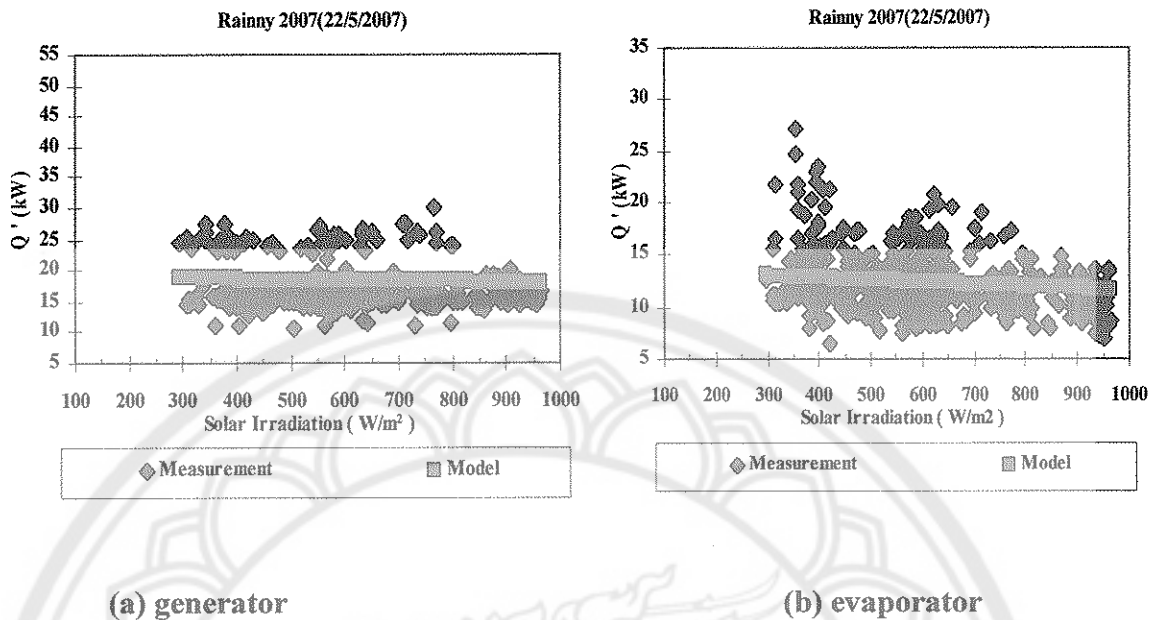


Figure 44 The result of running model with the fixed flow of water in the operated condition during rainy season.

Figure 43 and 44 showed the results when ran the summer and rainy season model comparison with the measurement through the generator and evaporator. Some notices had been gotten from these figures which explained the auxiliary usage was appearing during the operation.

4. The Technical Optimal Equation

Due to the hypothesis of this work, the always maximum COP was the purpose of this condition while the assumption describe the minimum heat losses that appeared by insulation all parts of system's components and no flow drop of water flow rate because of pump working. Therefore, the trapped energies could be generated by adjusted water flow rate, \dot{m} , as $x = f(y_1, y_2)$ when the $y_1 = \dot{m}$, $y_2 = \Delta T$ and $x = G_\beta$ so the calculation of the water flow rate would be hand on the sensible heat equation by mean of balancing energy as Eqs. 3-35 from the system's equations. The $\dot{Q}_{collector}$ and $\eta_{storage}$ was the input of the model as the energy supplying in each season. And the \dot{Q}_{evap} as the cooling load while the G_β was run that was shown on Table 6, 7 and 8 that shown the values of heat source and heat sink for generating the optimal water flow rate via the main components. The results of the simulation were used for

perdition the optimal \dot{m} and ΔT that generated the temperature of water via the main components. The simulation was consisting of three parts, energy supply, demand and reject.

Table 6 The heat source and heat sink of model during winter

Solar Irradiation ($G_{\beta} : \text{W/m}^2$)	Heat source		Heat sink ($\dot{Q}_{\text{evaporator}} : \text{kW}$)
	$\dot{Q}_{\text{collector}} : \text{kW}$	$\dot{Q}_{\text{storage}} : \text{kW}$	
200	6.4844	2.475095	-1.063
300	11.5044	4.736361	0.937
400	16.5244	7.298827	2.937
500	21.5444	10.16249	4.937
600	26.5644	13.32736	6.937
700	31.5844	16.79343	8.937
800	36.6044	20.56069	10.937
900	41.6244	24.62916	12.937
1000	46.6444	28.99882	14.937

Table 7 The heat source and heat sink of model during summer

Solar Irradiation ($G_{\beta} : \text{W/m}^2$)	Heat source		Heat sink ($\dot{Q}_{\text{evaporator}} : \text{kW}$)
	$\dot{Q}_{\text{collector}} : \text{kW}$	$\dot{Q}_{\text{storage}} : \text{kW}$	
200	7.25	2.58	-0.824
300	11.92	4.6	1.276
400	16.79	6.98	3.376
500	21.66	9.65	5.476
600	26.53	12.62	7.576
700	31.4	15.88	9.676
800	36.27	19.43	11.776
900	41.14	23.27	13.876
1000	46.01	27.4	15.976

Table 8 The heat source and heat sink of model during rainy season

Solar Irradiation ($G_{\beta} : \text{W/m}^2$)	Heat source		Heat sink
	$\dot{Q}_{\text{collector}} : \text{kW}$	$\dot{Q}_{\text{storage}} : \text{kW}$	($\dot{Q}_{\text{evaporator}} : \text{kW}$)
200	6.1211	43.34106	-0.744
300	11.0111	65.85298	1.396
400	15.9011	77.60691	3.536
500	20.7911	78.60283	5.676
600	25.6811	68.84076	7.816
700	30.5711	48.32068	9.956
800	35.4611	17.0426	12.096
900	40.3511	24.99347	14.236
1000	45.2411	77.78755	16.376

4.1 The Energy Supply

The energy supply consisted of two components, the first was solar collector and the other was hot water storage tank. The temperature of water in the supply part should be raised up when pass from collector through the storage before had been supplying. Figure 45 showed the simulation of temperature of water outlet from the solar collector, T_2 , during winter. The average G_{β} ranged 300 – 800 W.m^{-2} , so the optimal ΔT that generating the T_2 passed all average value was 6 °C. The appearing of the optimal \dot{m}_1 when the G_{β} was 600 W.m^{-2} should be 1.1 kg.s^{-1} while the T_2 was about 80°C. In summer, in Figure 46, the optimal ΔT was 8°C while the average G_{β} ranged 400 – 900 W.m^{-2} , so the optimal \dot{m}_1 was 0.8 kg.s^{-1} for generating T_2 was about 80 °C when the G_{β} was 600 W.m^{-2} . In Figure 47, rainy season, the optimal ΔT was 8°C for generating 80°C of T_2 supplying through the storage while the average G_{β} was 600 W.m^{-2} the adjusted \dot{m}_1 should be equal 0.8 kg.s^{-1} through the collector during rainy season.

In Figure 48, the optimal temperature would be pass through the storage tank in which the optimal \dot{m}_2 and ΔT should be generated the temperature of heat medium

inlet chiller, T_3 , not exceeds $95\text{ }^\circ\text{C}$ when the G_β was run. Generating the temperature supplies chiller, the optimal ΔT should be $4\text{ }^\circ\text{C}$ with the average G_β ranged $300 - 800\text{ W.m}^{-2}$. When the G_β was 600 W.m^{-2} , the optimal \dot{m}_2 should be 0.75 kg.s^{-1} for generated the T_3 was 75°C during winter. For summer in Figure 49, the optimal ΔT was $8\text{ }^\circ\text{C}$ while the average G_β was ranged $400 - 900\text{ W.m}^{-2}$. The T_3 was $80\text{ }^\circ\text{C}$ when G_β was 600 W.m^{-2} , the optimal \dot{m}_2 should be 0.5 kg.s^{-1} for generated maximum energy supply through the generator during summer.

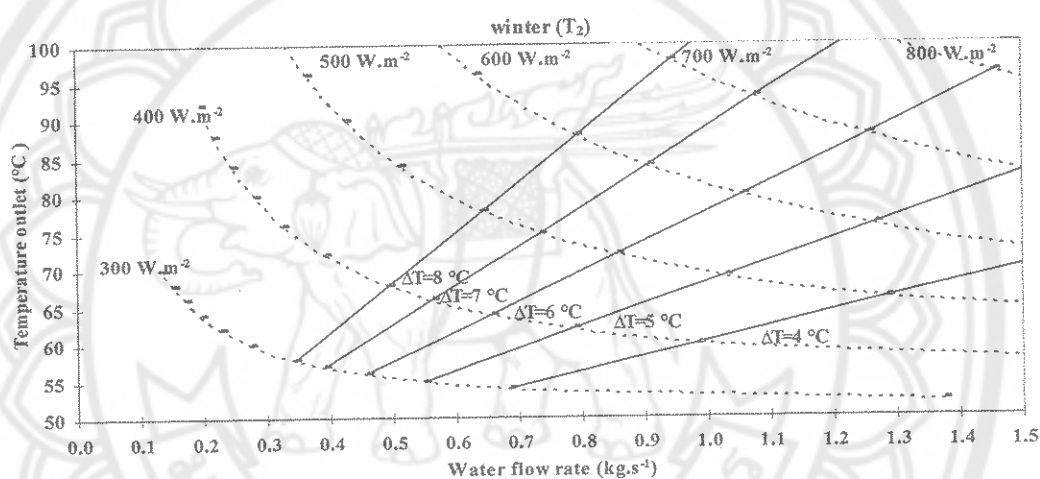


Figure 45 The temperature of hot water outlet the collector versus the water flow rate during winter

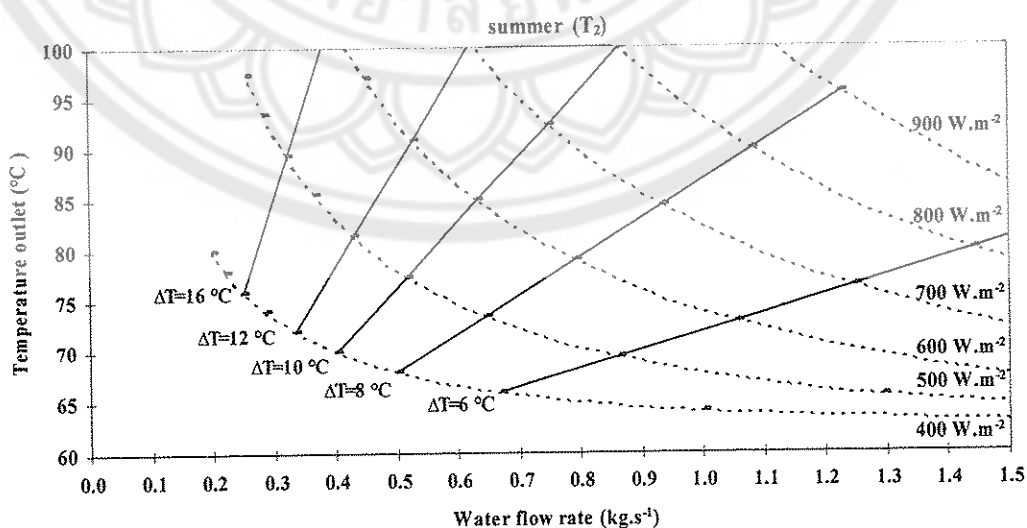


Figure 46 The temperature of hot water outlet the collector versus the water flow rate during summer

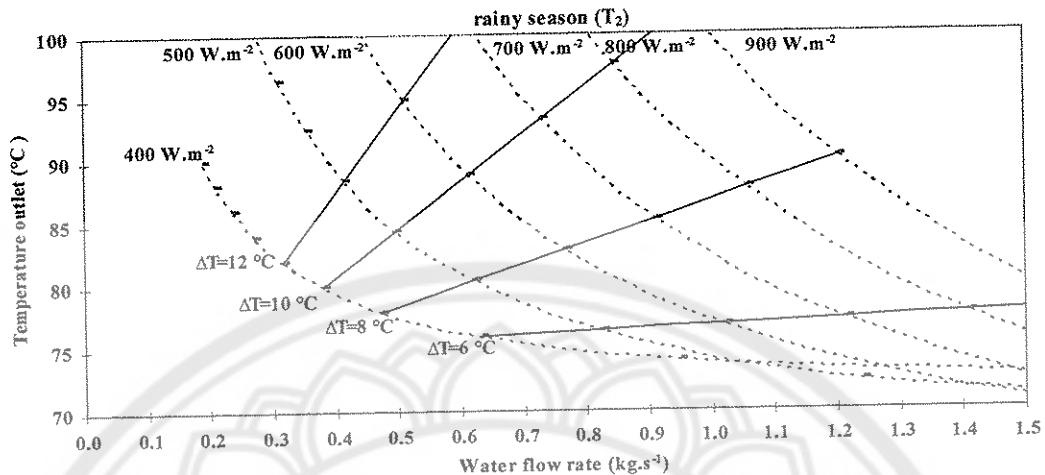


Figure 47 The temperature of hot water outlet the collector versus the water flow rate during rainy season

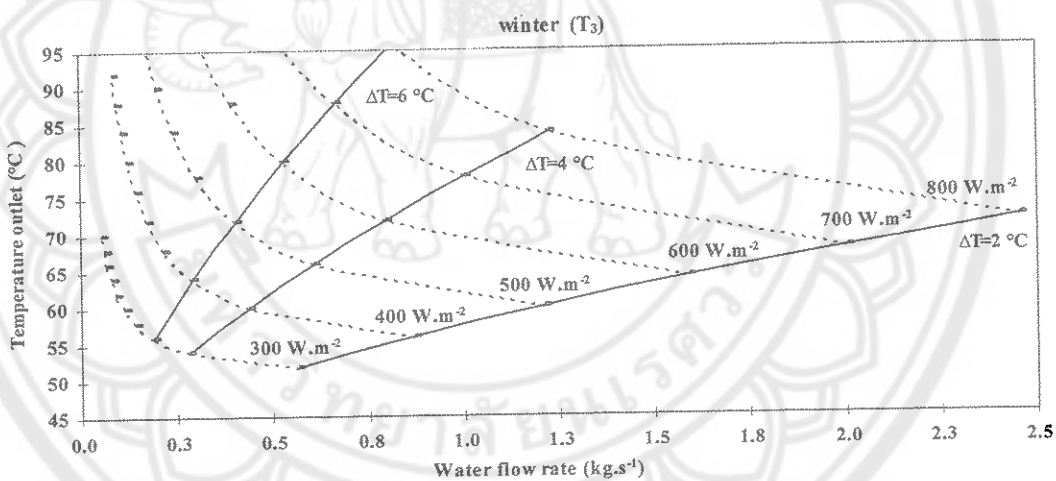


Figure 48 The temperature of hot water through the generator versus the water flow rate during winter

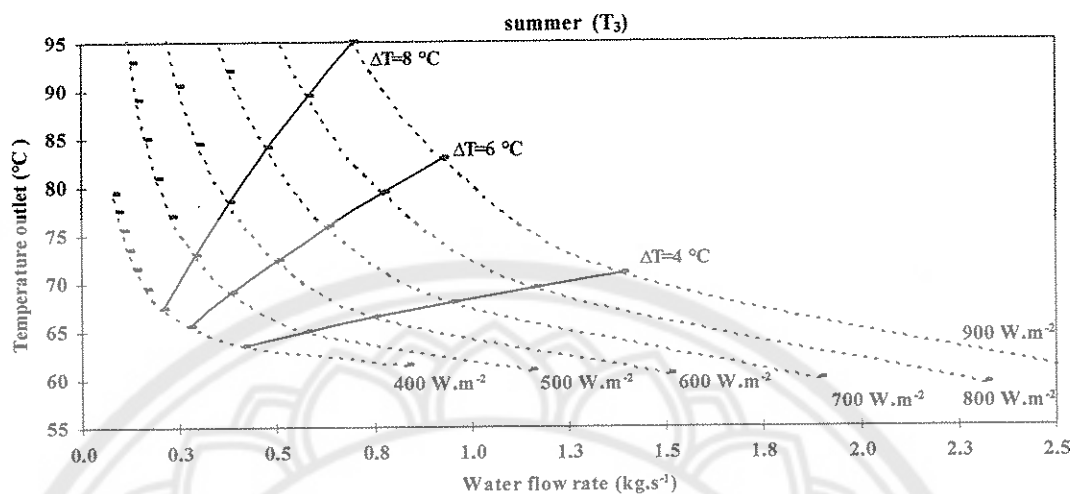


Figure 49 The temperature of hot water through the generator versus the water flow rate during summer

In Figure 50, both \dot{m}_2 and ΔT could not generate the optimal condition while the average G_β ranged 400 – 900 W.m^{-2} and the T_3 exceeded 95 $^\circ\text{C}$. The optimal situation did not appear in the graph by adjusting the \dot{m}_2 for the constant ΔT and maximum energy supply because this situation was using the auxiliary to heat up the temperature of water through the generator during the rainy season. The optimal \dot{m}_1 and \dot{m}_2 that generated the temperature of water via the collector and hot storage was written in the mathematic function with curves fitting method as shown in Table 9.

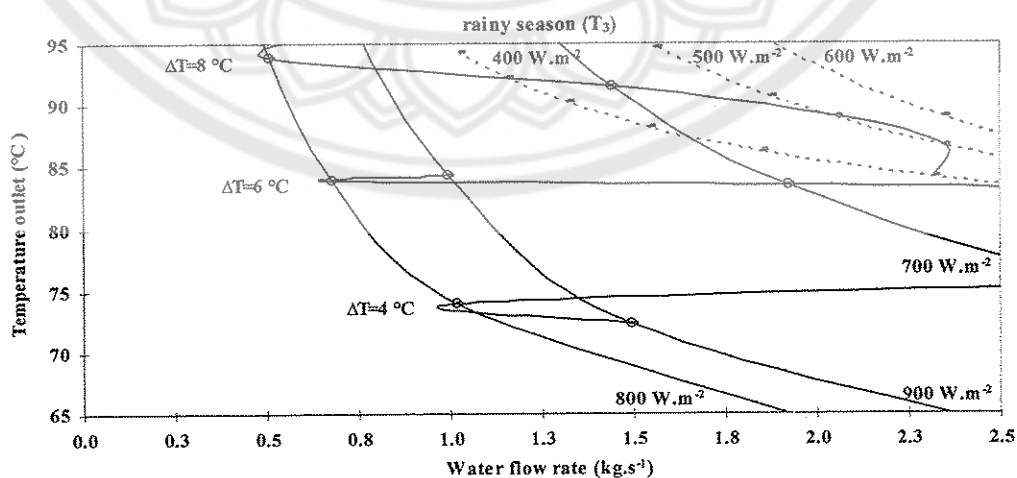


Figure 50 The temperature of hot water through the generator versus the water flow rate during the rainy season

Table 9 The mathematic function of energy supply in each season for generating the optimal temperature through the chiller

Hot storage		Collector	
Winter	R^2	Winter	R^2
$\Delta T = 4^\circ\text{C};$ $T_3 = 31.523\dot{m}_2 + 46.066$	0.99	$\Delta T = 6^\circ\text{C};$ $T_2 = 39.956\dot{m}_1 + 37.689$	1
Summer	R^2	Summer	R^2
$\Delta T = 8^\circ\text{C};$ $T_3 = 56.255\dot{m}_2 + 56.648$	0.99	$\Delta T = 8^\circ\text{C};$ $T_2 = 37.802\dot{m}_1 + 49.038$	1
Rainy Season	R^2	Rainy Season	R^2
Not in the optimal range		$\Delta T = 8^\circ\text{C};$ $T_2 = 16.565\dot{m}_1 + 70.131$	1

4.2 The Energy Demand

The optimal ΔT was generated the temperature of chilled water when the average G_β ranged 300 – 800 W.m^{-2} during the T_8 during winter as shown in Figure 51 was 2 °C. The optimal \dot{m}_4 should be 0.9 kg.s^{-1} when the G_β was 600 W.m^{-2} while the T_8 was 14 °C. For summer in Figure 52, the average G_β ranged 400 – 900 W.m^{-2} , the optimal condition would appeared in the graph by adjusting the \dot{m}_4 for generated the constant ΔT was 4 °C if the G_β was 600 W.m^{-2} , the optimal \dot{m}_4 would be 0.5 kg/s and the T_8 was 18 °C.

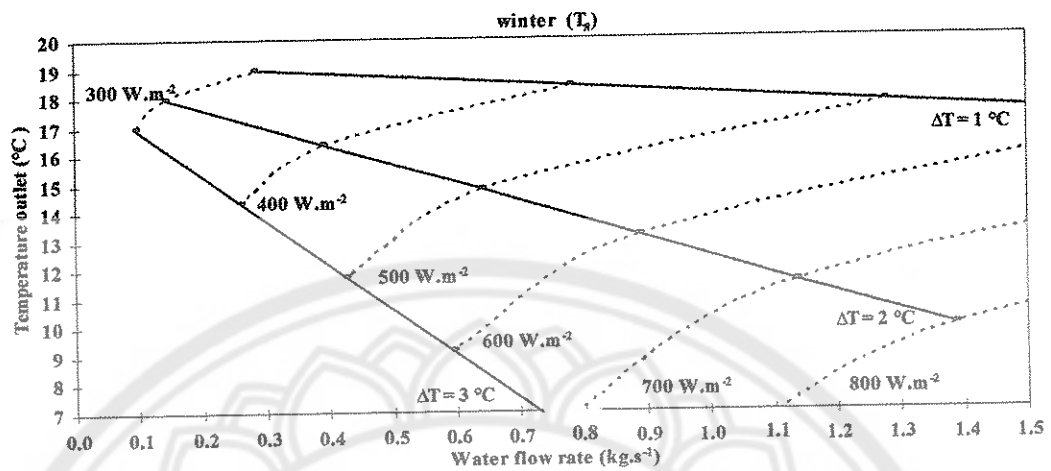


Figure 51 The temperature of chilled water through the building versus the water flow rate during winter

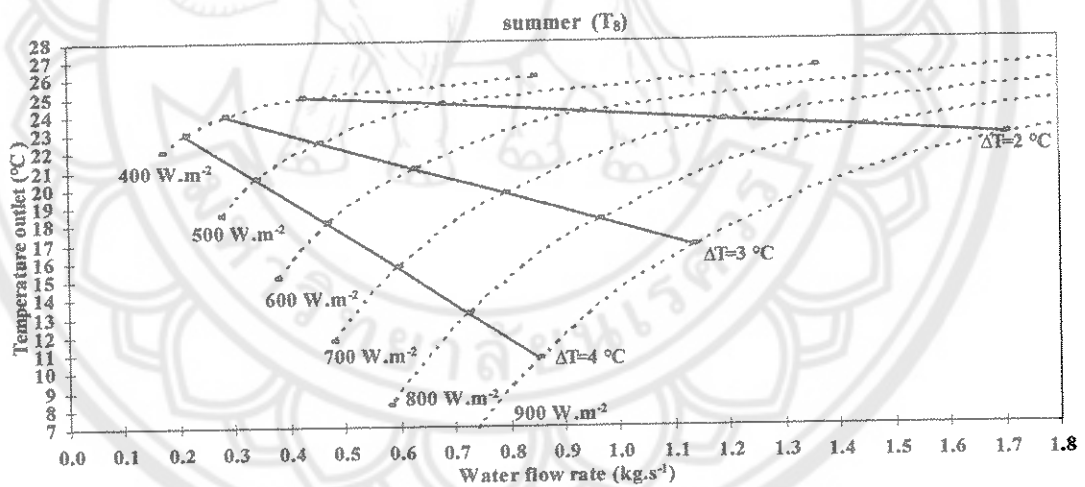


Figure 52 The temperature of chilled water through the building versus the water flow rate during summer

Both Figure 51 and 52 were non-usage auxiliary heat so that the temperature of chilled water was not good as usage auxiliary to rise up the temperature of water supplied through the chiller. The optimal ΔT was 4 °C while the G_p was 600 W.m⁻², the optimal \dot{m}_4 would be 0.5 kg.s⁻¹ and the T_s of chilled water was 18 °C.

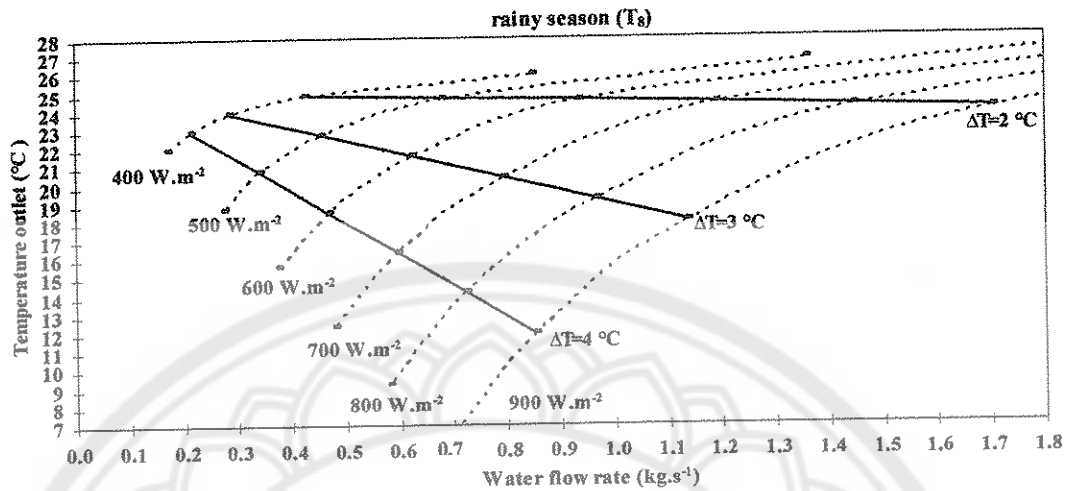


Figure 53 The temperature of chilled water through the building versus the water flow rate during rainy season.

4.3 The Energy Rejected

All energy that appeared during the process would be rejected by the working of cooling tower which was connected to the condenser and absorber. Figure 54-56 showed the prediction water temperature when operating with \dot{m} from the simulation. The optimal \dot{m}_3 was generate the temperature of cooling water should be 20 - 30 °C while the G_p was run.

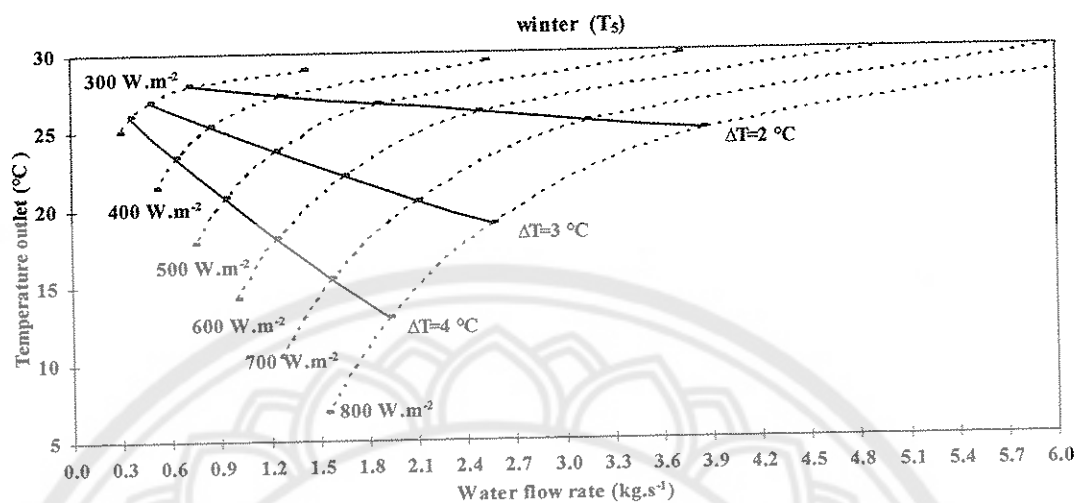


Figure 54 The temperature of cooling water for heat rejection versus the water flow rate during winter

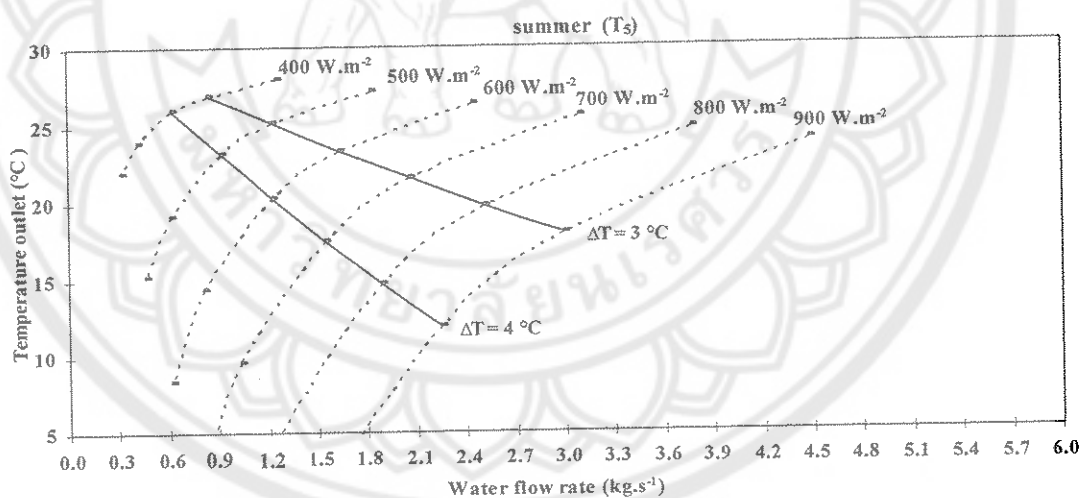


Figure 55 The temperature of cooling water for heat rejection versus the water flow rate during the summer season

In Figure 54, during winter, the average G_{β} ranged 300-800 W.m^{-2} , the optimal \dot{m}_3 , T_5 and ΔT of cooling water would be 1.2 kg.s^{-1} , 20 °C and 4 °C, respectively. On the

other hand, the average G_β ranged 400-900 $\text{W}\cdot\text{m}^{-2}$, T_5 was 20 $^\circ\text{C}$ with the ΔT was 4 $^\circ\text{C}$ and the optimal \dot{m}_3 was 1.2 $\text{kg}\cdot\text{s}^{-1}$ in 600 $\text{W}\cdot\text{m}^{-2}$ of G_β in summer in Figure 55. In Figure 56, the optimal condition did not appeared in rainy season by adjusting the \dot{m}_3 for generated the constant ΔT and maximum energy supply because this situation was used the auxiliary to heat up the temperature of water through the generator during rainy season.

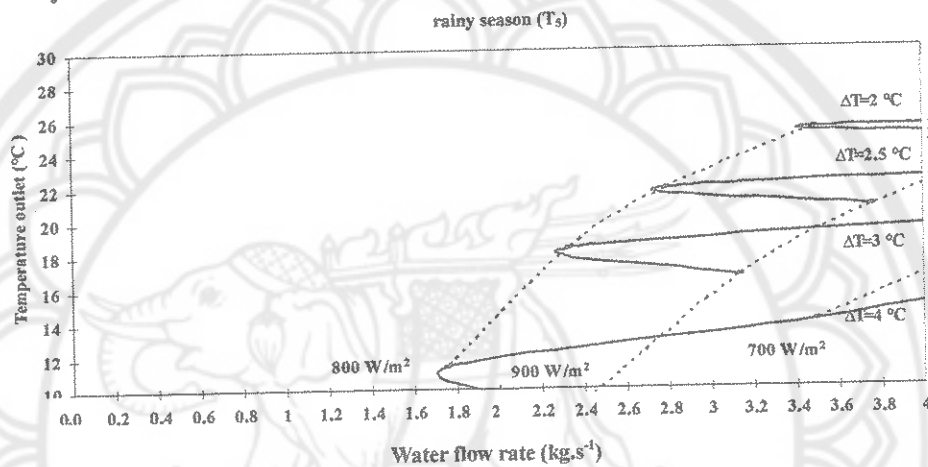


Figure 56 The temperature of cooling water for heat rejection versus the water flow rate during rainy season

Table 10 The mathematic function of energy demand and rejected in each season for generating the optimal temperature through the chiller

Load		Cooling Tower	
Winter	R^2	Winter	R^2
$\Delta T = 2^\circ\text{C};$ $T_8 = -6.477\dot{m}_4 + 18.911$	1	$\Delta T = 4^\circ\text{C};$ $T_5 = -8.346\dot{m}_3 + 28.687$	0.99
Summer		Summer	
$\Delta T = 4^\circ\text{C};$ $T_8 = -19.16\dot{m}_4 + 27.046$	1	$\Delta T = 4^\circ\text{C};$ $T_5 = -8.667\dot{m}_3 + 31.181$	0.99
Rainy Season		Rainy Season	
$\Delta T = 4^\circ\text{C};$ $T_8 = -17.127\dot{m}_4 + 26.619$	1	Not in the optimal range	

The water temperature via the main components in each season was the output from simulation which was the optimal water flow rate and the differential temperature. These output was used as guideline for the optimal operation for generated the maximum actual COP.

5. The SIMULINK, MATLAB Model

The next step, all component models were written by SIMULINK, MATLAB for guideline the operation of this system which required the maximum actual \dot{Q} and COP. The results of the prediction were the optimal \dot{m} and T via the main components. Figure 57 showed the technical optimization model during winter that written by SIMULINK, MATLAB, to find out the condition that the chiller could generated the maximum actual COP. The input of the model was the solar irradiation, G_β , was 300 – 1000 W.m^{-2} when input G_β was put in number (1) then the output was COP which was calculated from the relationship between \dot{Q}_{gen} and \dot{Q}_{evap} was shown on number (2). Number (3) and (4) showed the value of \dot{m}_1 and T_2 and number (5) and (6) was \dot{m}_2 and T_3 that was used for generating maximum $\dot{Q}_{collector}$ and \dot{Q}_{gen} , respectively. The \dot{m}_4 and T_8 was displayed on number (7) and (8) by mean of maximum cooling capacity, \dot{Q}_{evap} that produced by the chiller. \dot{m}_3 and T_5 was displayed on number (9) and (10) base on the relation of $\dot{Q}_{rej} = \dot{Q}_{gen} + \dot{Q}_{evap}$ in each season.

This situation of the technical optimal model was written in from of the mass balance equation as the Eqs. 3-28.

$$\text{Winter :} \quad (6\dot{m}_1 + 4\dot{m}_2) + 2\dot{m}_4 = 4\dot{m}_3 \quad (4-1)$$

$$\text{Summer :} \quad (8\dot{m}_1 + 8\dot{m}_2) + 4\dot{m}_4 = 4\dot{m}_3 \quad (4-2)$$

$$\text{Rainy season:} \quad (8\dot{m}_1 + \dot{m}_2\Delta T_{3-4}) + 4\dot{m}_4 = \dot{m}_3\Delta T_{6-5} \quad (4-3)$$

The ΔT_{3-4} and ΔT_{6-5} was not in the optimal range both the temperature of heat medium inlet the chiller, T_3 , exceeded 95 °C and limited working of pump during rainy season model.

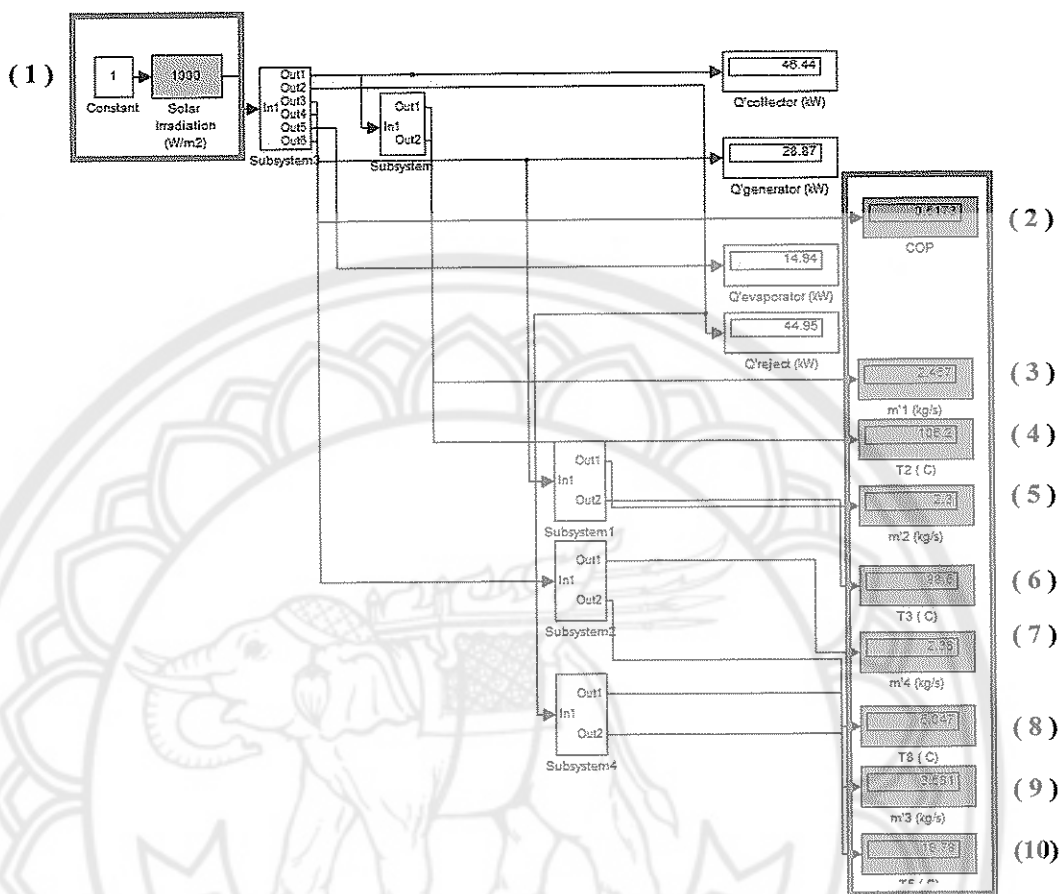


Figure 57 The technical optimization model during winter

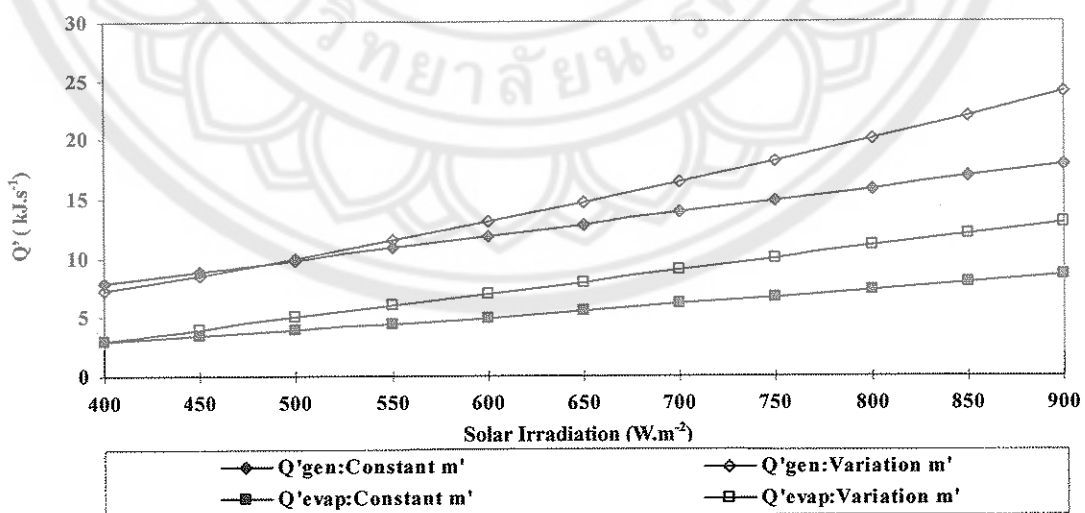


Figure 58 The result of running fixed and varied water flow rate model during summer

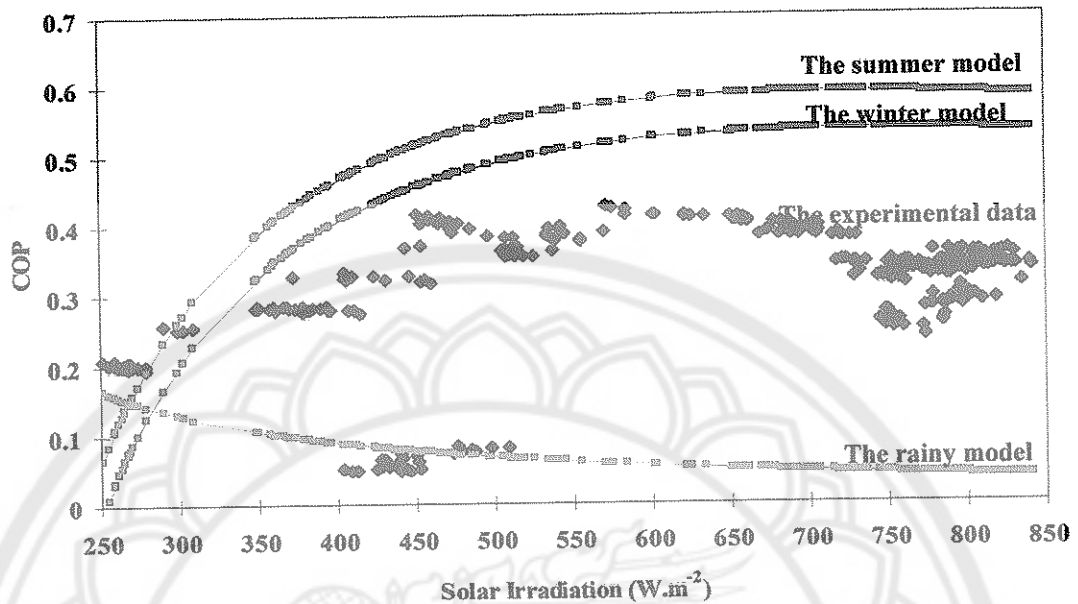


Figure 59 The comparison of COP versus solar irradiation between the experiment data and the model in each season during a year.

To compare the energy supply and demand that generated by fixed and varied water flow rate from running the mathematic model. Both were constructed by curve fitting method one was come from the experimental data the other was simulation. In Figure 58, the variation \dot{m} situation could generate higher both \dot{Q}_{gen} and \dot{Q}_{evap} than the fix done during the summer season. Same as the prediction of the variation of water flow rate by mean of balancing heat sink and heat source was suitable for the non-auxiliary usage condition shown that the actual COP in the Figure 59 when fix the value of \dot{m} was the measurement evaluation written as black points was lower than other line was the result of simulation of seasonal model when adjusting the water flow rate. Using both energy sources for generating the higher water temperature the lower COP was appear because of unbalance between the huge heat source and the few heat loads.

The Economic Equation and Condition

The capital costs came to a total of 2,974,846 Baht (85,000 U.S. Dollar) with the calculated detail as shown in Table 11. The analysis used SLCCA method base on assumption of the life time was 20 year, the operation period was 8 hour per day that follows in Table 12.

Table 11 The capital costs for SERT Energy Park cooling system.

Components	Estimated Specific Cost	Life Time (Year)*
Absorption Chiller	40,000 Baht.kW ⁻¹	20
Solar Collector Array	13,000 Baht. m ⁻²	20
Auxiliary Heater	-	10
Heat Storage Unit	-	20
Cool Storage Unit	-	20
Cooling Tower	180 Baht.kW ⁻¹	20
Fan Coil (4Units)	1,200 Baht.kW ⁻¹	10
Pump (4 Units)	20,000 Baht.kW ⁻¹	20
Labor/ Transportation	-	-

1 U.S. Dollar = 35 Baht (Bank of Thailand, 2007), * (ASHRAE Handbook, 2003)

The results showing the monthly techno-economic analysis were given in Table 13. The solar cooling system provided the daily average useful cold, Q_{cold} , was 132.32 kWh with the daily average driving heat, Q_{heat} , was 370.64 kWh in which a half of thermal supplied by solar energy, $SOLF_{the} = 0.59$. The daily average COP was 0.34 while the daily average ambient temperature, T_a , high water temperature inlet chiller, T_3 , and cooled water temperature outlet evaporator, T_8 , was 32, 72 and 15 C°, respectively. The calculation of SLCCA was about 8 Baht.kWh⁻¹ or 64.24 Baht per day (1.84 U.S. Dollar per day) for this available system. The rating supplied by the manufacturer showed a COP at nominal conditions equal to 0.70, the measurement values of the daily average actual COP was 0.34. The improvement depended on the thermal performance, COP, if the maximum COP was required for the continuous

operation, COP=0.7, the payment was about 3 Baht.kWh⁻¹ for each SOLF_{the}.

Table 12 The calculated extent for economic performance analysis
(Yongprayun, Ketjoy, and Rakwichian, 2007, unpagged).

Description						
Capital Cost (C_A)		2,974,846 Baht				
Annual Maintenance Cost		1	% of C_A			
Annual Running Cost (C_R)						
- Electric Cost						
COP = 0.2		2.10	Baht.kWh ⁻¹			
COP = 0.3		1.40	Baht.kWh ⁻¹			
COP = 0.4		1.05	Baht.kWh ⁻¹			
COP = 0.5		0.84	Baht.kWh ⁻¹			
COP = 0.6		0.70	Baht.kWh ⁻¹			
COP = 0.7		0.60	Baht.kWh ⁻¹			
- LPG Cost Baht.kWh ⁻¹						
	COP = 0.2	COP = 0.3	COP = 0.4	COP = 0.5	COP = 0.6	COP = 0.7
SOLF _{the} = 0.4	1.39	0.93	0.70	0.56	0.46	0.40
SOLF _{the} = 0.5	1.16	0.78	0.58	0.47	0.39	0.33
SOLF _{the} = 0.6	0.93	0.62	0.46	0.37	0.31	0.26
SOLF _{the} = 0.7	0.69	0.46	0.35	0.28	0.23	0.20
SOLF _{the} = 0.8	0.46	0.31	0.23	0.19	0.15	0.13
SOLF _{the} = 0.9	0.23	0.15	0.12	0.09	0.08	0.07
Replacement Cost (C_{RE}) in the last 10 year						
-Auxiliary Heater		0.15	Baht.kWh ⁻¹			
-Fan Coil (4Units)		0.05	Baht.kWh ⁻¹			
Salvage Cost (C_S)		5	% of C_A			
Discount Rate (i)		6	%			
Life Time (n)		20	Years			

Table 13 Techno-economic analysis of 35 kW solar cooling system, Thailand

Month	\bar{G}_β (kWh.m ⁻²)	T_3 (C°)	T_8 (C°)	T_a (C°)	Q_{heat} (kWh)	Q_{cold} (kWh)	$Q_{auxiliary}$ (kWh)	COP	$SOLF_{the}$	SLCCA (Baht.kWh ⁻¹)
Jan	5.10	73	11	21	412.64	200.00	211.68	0.48	0.49	4.18
Feb	4.90	70	16	30	336.40	161.04	108.72	0.47	0.68	4.13
Mar	4.90	71	18	34	421.76	125.60	114.40	0.30	0.73	6.79
Apr	5.55	75	19	34	450.80	110.24	186.48	0.24	0.81	10.05
May	5.40	74	15	34	380.08	110.64	186.48	0.29	0.51	10.45
Jun	5.20	70	17	33	308.00	83.44	152.00	0.27	0.51	10.45
Jul	5.10	73	14	33	337.36	126.64	148.16	0.38	0.56	6.97
Aug	4.30	63	20	32	347.36	89.20	160.96	0.26	0.54	10.45
Sep	5.45	69	17	34	399.60	101.44	186.48	0.25	0.53	10.45
Oct	5.20	74	13	34	422.32	195.68	150.64	0.46	0.64	5.16
Nov	5.00	74	15	34	500.56	187.36	170.64	0.37	0.65	6.88
Dec	4.65	74	18	31	419.12	96.88	211.28	0.23	0.50	10.45
\bar{X}	5.10	72	15	32	394.64	132.32	157.20	0.34	0.59	8.03

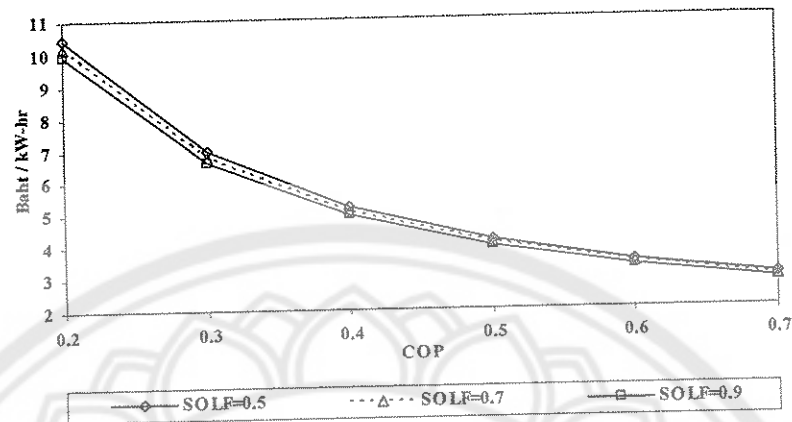


Figure 60 The sensible analysis of COP and SOLF_{the} to generate the lowest SLCCA

The sensible analysis of both COP and SOLF_{the} with the Specific Life Cycle Cost Analysis (SLCCA), Net Present Value (NPV), Internal Rate of Return (IRR), Payback Period (PB) and Benefit-Cost ratio (B/C) were shown in Figure 60 – 63. Changing of COP from 0.3 to 0.6 decreasing SLCCA about 50% from 6 Bath to 3 Bath in each SOLF_{the} in Figure 60. In Figure 61, the maximum IRR was about 9% when the COP came through 0.7 in each SOLF_{the}.

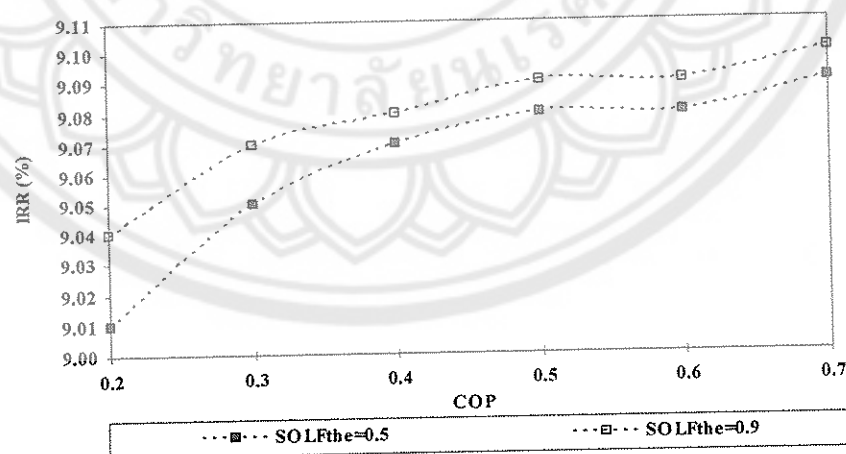


Figure 61 The sensible analysis of COP and SOLF_{the} to generate the highest IRR (%)

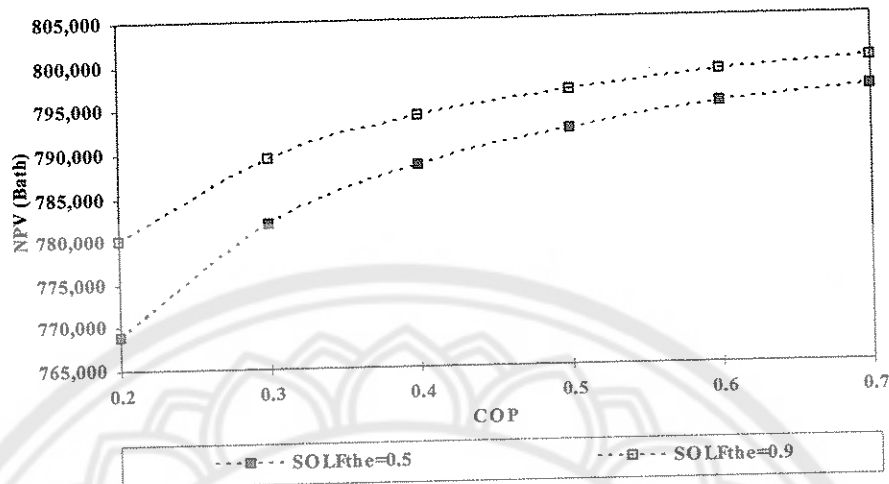


Figure 62 The sensible analysis of COP and SOLF_{the} to generate the highest NPV

In Figure 62, increasing of COP and SOLF_{the} effect to the increasing of NPV when the COP was changed from 0.3 to 0.6, the NPV was increased about 0.3% with the same SOLF_{the}. While the SOLF_{the} was increased from 0.5 to 0.9, the NPV was changed about 0.9 % with the same COP in each season.

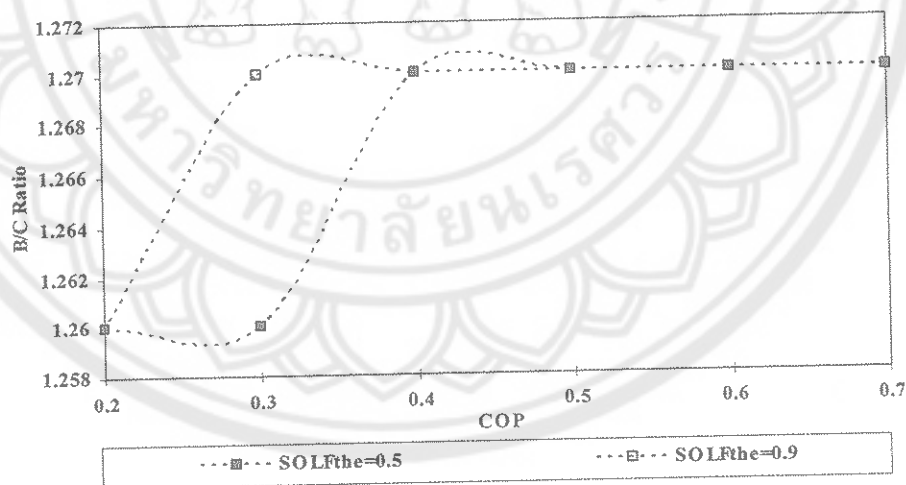


Figure 63 The sensible analysis of COP and SOLF_{the} to generate the highest B/C Ratio

The benefit-cost ratio, B/C Ratio, was increased when the COP and SOLF_{the} was run from 0.2 to 0.7 and from 0.3 to 0.9, respectively. The beginning of maximum B/C Ratio was 1.27 when the COP and SOLF_{the} was 0.3 and 0.9, respectively. Both

COP and $SOLF_{the}$ did not effect with the PB. The PB was 13.8 year in each COP and $SOLF_{the}$.

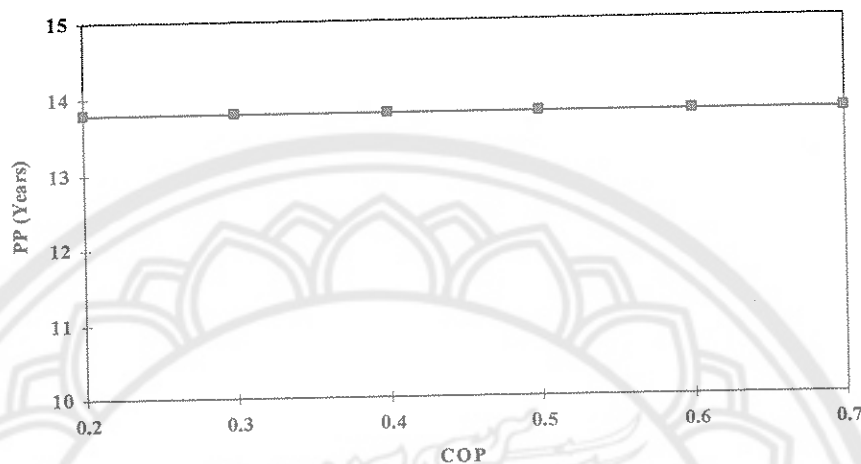


Figure 64 The sensible analysis of COP and $SOLF_{the}$ to generate the shortest PB

For the hypothesis of this work, the lowest total SLCCA appeared as same as the highest NPV, IRR and B/C Ratio when the maximum actual COP was produced as shown in Figure 60-63. There was no reason to turn this cooling system into a minimum COP since this would increased the reliability and decreased the cost of the operated system by mean of the higher COP, the lower SLCCA together with the higher NPV, IRR and B/C Ratio appeared. Therefore, the simulation model should be a powerful tool for solar cooling both development and testing of control strategies. The economic mathematic functions were shown in Table 15. The $SOLF_{the}$ of the non-usage auxiliary heat situation was 0.9 while the usage was 0.5 that base on the evaluations of the experimental data.

Table 14 The economic optimal equation for solar cooling at SERT

List	Winter	Summer	Rainy Season
SLCCA = f(COP)	SLCCA=32.34COP ² -42.35COP+16.83 R ² =0.99		SLCCA=34.125COP ² -44.66COP+17.742 R ² =0.99
IRR = f(COP)	IRR=-0.25COP ² +0.33COP+8.99 R ² =0.96		IRR=-0.42COP ² +0.51COP+8.93 R ² =0.97
NPV = f(COP)	NPV=-91252COP ² +119436COP+760512 R ² =0.99		NPV= -127670COP ² +167093COP+741583 R ² =0.99
B/C Ratio = f(COP)	B/C Ratio=-0.09COP ² +0.09COP+1.25 R ² =0.85		B/C Ratio=-0.07COP ² +0.09COP+1.24 R ² =0.86
PB = f(COP)	PB= 13.8 R ² =1		PB= 13.8 R ² =1

The Optimal Operation and Condition

Due to the Purpose of this work was optimization both the technique and economy of LiBr – H₂O solar absorption cooling system in Thailand. The optimal technical equations were constructed by the relationship between the variation of water flow rate via the main component, differential temperature and the tilt solar irradiation by mean of improving the actual COP. The optimal economic equation were constructed by the variation both of the coefficient of performance (COP) was 0.35 - 0.65 and the solar fraction (SOLF_{the}) was 0.5 – 1 to generate the lowest of SLCCA, the shorten time for pay back period (PB), and the highest rate of return (IRR), net present value (NPV), computation of B/C ratio for a single investment. Normally, the economic analysis factor was IRR while the technical analysis factor was COP. Therefore, the comparison of IRR and COP between the simulation and the measurement during winter and summer as shown in Figure 65 and 66.

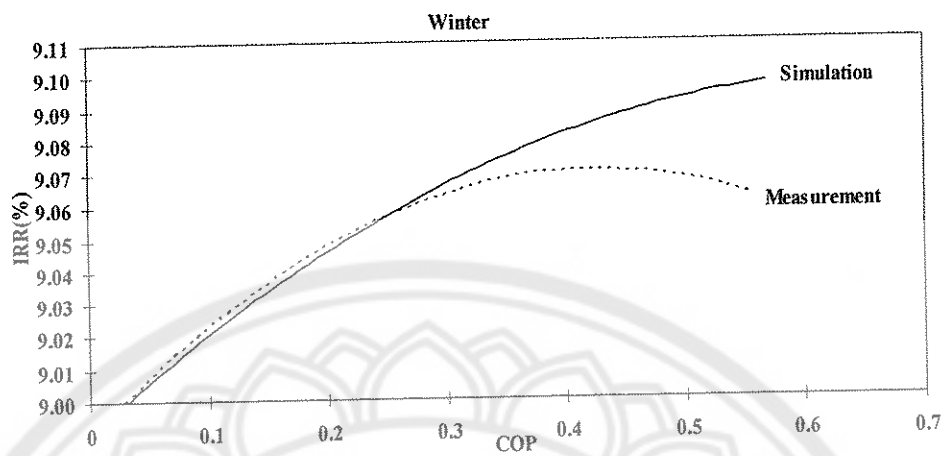


Figure 65 The comparison of IRR versus COP between the simulation and the measurement during winter

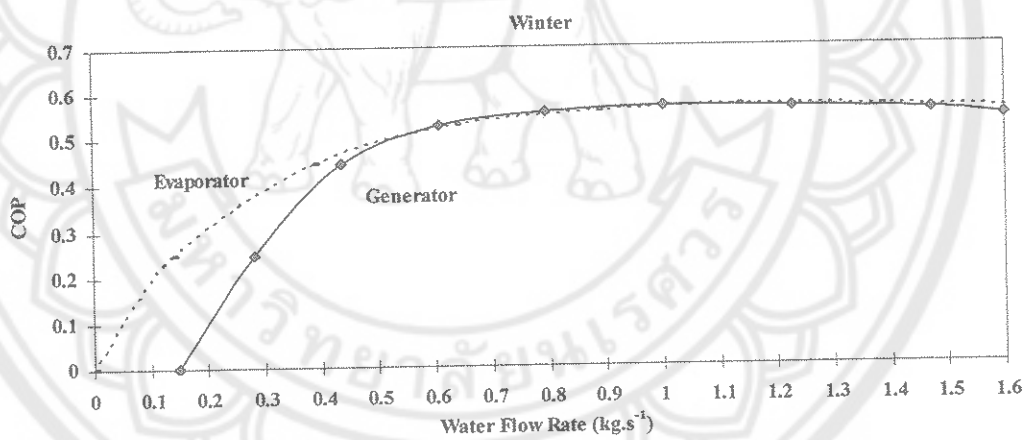


Figure 66 The comparison of COP versus water flow rate via the generator and the evaporator during winter

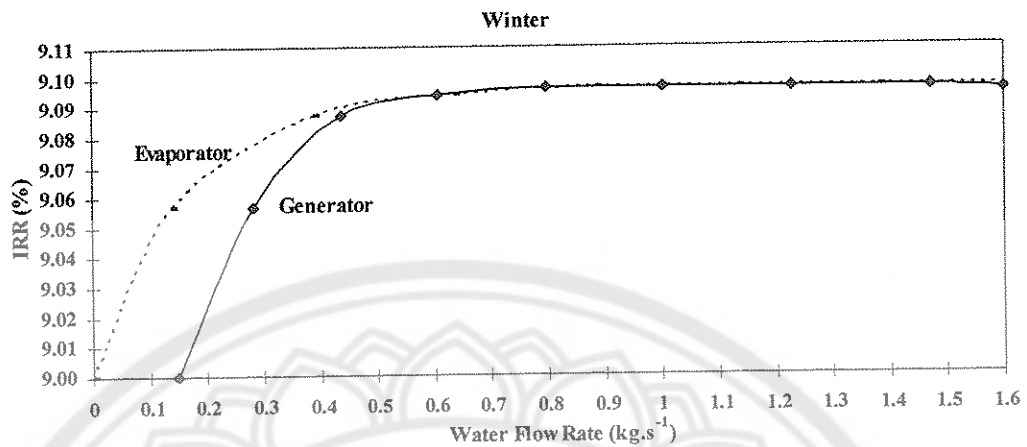


Figure 67 The comparison of IRR versus water flow rate via the generator and the evaporator during winter

In Figure 65, higher COP was generate higher IRR. In winter, the variation of water flow could generate higher IRR than fixed flow at the end of the operation. The simulation could predict the optimal flow rate thus the maximum actual COP was always appear when adjusted the water flow rate with the optimal value. In Eqs. (3-17), the COP was the divided result between \dot{Q}_{evap} and \dot{Q}_{gen} which was explained as the mathematic equation in Eqs. (3-12) and (3-13). Therefore, the optimal condition was plotted between COP, IRR and the variation of water flow rate via the evaporator, \dot{m}_4 and generator, \dot{m}_2 .

In Figure 66, the prediction of the optimal condition during winter was appear when \dot{m}_4 and \dot{m}_2 ranged 0.6-1 kg.s⁻¹ for generated the maximum actual COP while the maximum IRR was appear when adjusted \dot{m}_4 and \dot{m}_2 ranged 0.5-0.8 kg.s⁻¹ as shown in Figure 67. Therefore, \dot{m}_4 and \dot{m}_2 did not exceed 1 kg.s⁻¹ in winter. If the variation was over than this, higher energy consumption for water pumping would be appear while the IRR did not increase.

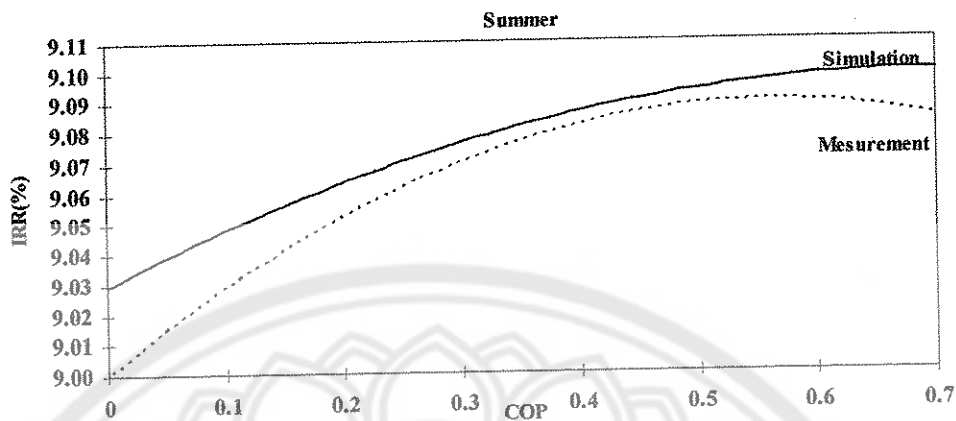


Figure 68 The comparison of IRR versus COP between the simulation and the measurement during summer

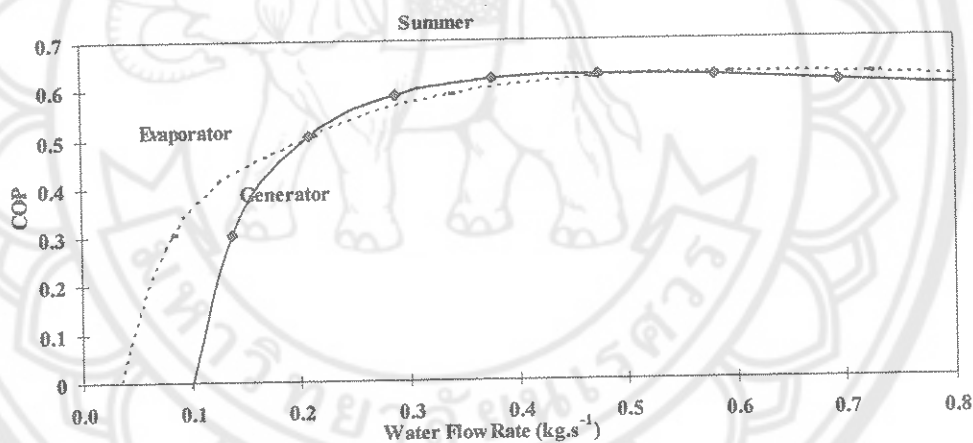


Figure 69 The comparison of COP versus water flow rate via the generator and the evaporator during summer

Throughout the operation in summer, the variation of \dot{m}_4 and \dot{m}_2 could generate higher IRR than the fixed flow situation as shown in Figure 68. Thus, the prediction of the optimal condition during summer was appear when \dot{m}_4 and \dot{m}_2 ranged 0.2-0.5 kg.s^{-1} for generated the maximum actual COP as shown in Figure 69 while the maximum IRR was appear when adjusted \dot{m}_4 and \dot{m}_2 ranged 0.1-0.4 kg.s^{-1} as shown in Figure 70. It meant \dot{m}_4 and \dot{m}_2 did not exceed 0.5 kg.s^{-1} by mean of the optimization both technically and economically.

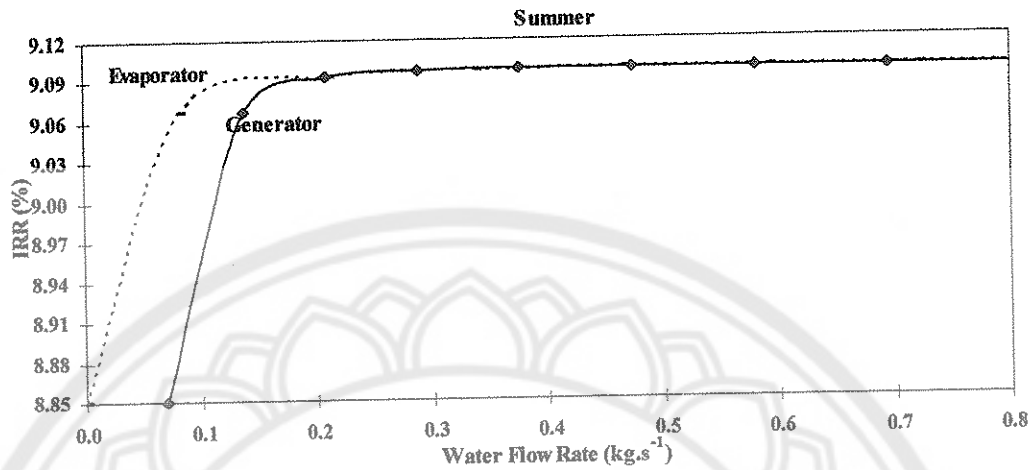


Figure 70 The comparison of IRR versus water flow rate via the generator and the evaporator during summer

The optimal water flow rate via the main components could generate the maximum actual COP and IRR during winter and summer when operation followed this condition as in Table 15.

Table 15 The optimal equations for solar cooling at SERT

Winter	Summer
Generator	Generator
$\dot{m} < 0.6 \text{ kg.s}^{-1} ; \text{COP} = -6.30\dot{m}^2 + 6.61\dot{m} - 1.18 (R^2 = 0.98)$	$\dot{m} < 0.2 \text{ kg.s}^{-1} ; \text{COP} = -42.76\dot{m}^2 + 17.65\dot{m} - 1.32 (R^2 = 1)$
$\text{IRR} = -4.95\dot{m}^2 + 3.76\dot{m} + 8.39 (R^2 = 1)$	$\text{IRR} = -0.01\dot{m}^2 + 0.01\dot{m} + 9.09 (R^2 = 0.86)$
$\dot{m} \geq 0.6 \text{ kg.s}^{-1} ; \text{COP} = -0.09\dot{m}^2 + 0.24\dot{m} + 0.42 (R^2 = 0.88)$	$\dot{m} \geq 0.2 \text{ kg.s}^{-1} ; \text{COP} = -0.46\dot{m}^2 + 0.51\dot{m} + 0.48 (R^2 = 0.87)$
$\text{IRR} = -0.01\dot{m}^2 + 0.03\dot{m} + 9.08 (R^2 = 0.85)$	$\text{IRR} = -20.60\dot{m}^2 + 7.49\dot{m} + 8.43 (R^2 = 1)$
Evaporator	Evaporator
$\dot{m} < 0.6 \text{ kg.s}^{-1} ; \text{COP} = -2.16\dot{m}^2 + 2.30\dot{m} - 0.07 (R^2 = 0.99)$	$\dot{m} < 0.2 \text{ kg.s}^{-1} ; \text{COP} = -26.14\dot{m}^2 + 9.28\dot{m} - 0.29 (R^2 = 1)$
$\text{IRR} = -1.53\dot{m}^2 + 0.94\dot{m} + 8.96 (R^2 = 1)$	$\text{IRR} = -0.01\dot{m}^2 + 0.01\dot{m} + 9.09 (R^2 = 0.92)$
$\dot{m} \geq 0.6 \text{ kg.s}^{-1} ; \text{COP} = -0.08\dot{m}^2 + 0.22\dot{m} + 0.42 (R^2 = 0.94)$	$\dot{m} \geq 0.2 \text{ kg.s}^{-1} ; \text{COP} = -0.33\dot{m}^2 + 0.44\dot{m} + 0.48 (R^2 = 0.93)$
$\text{IRR} = -0.01\dot{m}^2 + 0.01\dot{m} + 9.09 (R^2 = 0.93)$	$\text{IRR} = -11.38\dot{m}^2 + 3.55\dot{m} + 8.85 (R^2 = 1)$